Genetic tool development in marine protists:

Emerging model organisms for experimental cell biology

Drahomíra Faktorová[1,#,*], R. Ellen R. Nisbet[2,#], José A. Fernández Robledo[3,#], Elena Casacuberta[4,#], Lisa Sudek[5,#], Andrew E. Allen[6,7], Manuel Ares Jr.[8], Cristina Aresté[4], Cecilia Balestreri[9], Adrian C. Barbrook[2], Patrick Beardslee[10], Sara Bender[11], David S. Booth[12], François-Yves Bouget[13], Chris Bowler[14], Susana A. Breglia[15], Colin Brownlee[9], Gertraud Burger[16], Heriberto Cerutti[10], Rachele Cesaroni[17], Miguel A. Chiurillo[18], Thomas Clemente[10], Duncan B. Coles[3], Jackie L. Collier[19], Elizabeth C. Cooney[20], Kathryn Coyne[21], Roberto Docampo[18], Christopher L. Dupont[7], Virginia Edgcomb[22], Elin Einarsson[2], Pía A. Elustondo[15,$], Fernan Federici[23], Veronica Freire-Beneitez[24,25], Nastasia J. Freyria[3], Kodai Fukuda[26], Paulo A. García[27], Peter R. Girguis[28], Fatma Gomaa[28], Sebastian G. Gornik[29], Jian Guo[5,8], Vladimír Hampl[30], Yutaka Hanawa[31], Esteban R. Haro-Contreras[15], Elisabeth Hehenberger[20], Andrea Highfield[9], Yoshihisa Hirakawa[31], Amanda Hopes[32], Christopher J. Howe[2], Ian Hu[2], Jorge Ibañez[23], Nicholas A.T. Irwin[20], Yuu Ishii[33], Natalia Ewa Janowicz[30], Adam C. Jones[11], Ambar Kachale[1], Konomi Fujimura-Kamada[34], Binnypreet Kaur[1], Jonathan Z. Kaye[11], Eleanna Kazana[24,25], Patrick J. Keeling[20], Nicole King[12], Lawrence A. Klobutcher[35], Noelia Lander[18], Imen Lassadi[2], Zhuhong Li[18], Senjie Lin[35], Jean-Claude Lozano[13], Fulei Luan[10], Shinichiro Maruyama[33], Tamara Matute[23], Cristina Miceli[36], Jun Minagawa[34,37], Mark Moosburner[6,7], Sebastián R. Najle[4,38], Deepak Nanjappa[21], Isabel C. Nimmo[2], Luke Noble[39,**], Anna M.G. Novák Vanclová[30], Mariusz Nowacki[17], Isaac Nuñez[23], Arnab Pain[40,41], Angela Piersanti[36], Sandra Pucciarelli[36], Jan Pyrih[1,24,30], Joshua S. Rest[42], Mariana Rius[19], Deborah Robertson[43], Albane Ruaud[23,***], Iñaki Ruiz-Trillo[4,44,45], Monika A. Sigg[12], Pamela A. Silver[46,47], Claudio H. Slamovits[15], G. Jason Smith[48], Brittany N. Sprecher[35], Rowena Stern[9], Estienne Swart[17,&], Anastasios Tsaousis[24,25], Lev Tsypin[49,50],

Aaron Turkewitz[49], Jernej Turnšek[6,7,46,47], Matus Valach[16], Valérie Vergé[13], Peter von Dassow[23,51], Tobias von der Haar[24], Ross F. Waller[2], Lu Wang[52], Xiaoxue Wen[10], Glen Wheeler[9], April Woods[48], Huan Zhang[35], Thomas Mock[32,*], Alexandra Z. Worden[5,53,*] & Julius Lukeš[1,*]

[#]Equal contribution

[*]Corresponding authors: dranov@paru.cas.cz (DF); t.mock@uea.ac.uk (TM); azworden@geomar.de (AZW); jula@paru.cas.cz (JL)

[1]*Institute of Parasitology, Biology Centre, Czech Academy of Sciences and Faculty of Sciences, University of South Bohemia, České Budějovice, Czech Republic*

[2]*Department of Biochemistry, University of Cambridge, Cambridge, UK*

[3]*Bigelow Laboratory for Ocean Sciences, East Boothbay, USA*

[4]*Institut de Biologia Evolutiva, CSIC-Universitat Pompeu Fabra, Barcelona, Spain*

[5]*Monterey Bay Aquarium Research Institute, Moss Landing, USA*

[6]*Integrative Oceanography Division, Scripps Institution of Oceanography, University of California, San Diego, USA*

[7]*Microbial and Environmental Genomics, J. Craig Venter Institute, La Jolla, USA*

[8]*Molecular, Cell and Developmental Biology, University of California, Santa Cruz, USA*

[9]*The Marine Biological Association, Plymouth and School of Ocean and Earth Sciences, University of Southampton, UK*

[10]*School of Biological Sciences, University of Nebraska, Lincoln, USA*

[11]*Gordon and Betty Moore Foundation, Palo Alto, USA*

[12]*Department of Molecular and Cell Biology, University of California, Berkeley, USA*

[13]*Sorbonne Université, CNRS UMR7621, Observatoire Océanologique, Banyul sur Mer, France*

[14]*Institute de Biologie de l'ENS, Département de biologie, École Normale Supérieure, CNRS, INSERM, Paris, France*

[15]*Centre for Comparative Genomics and Evolutionary Bioinformatics, Dalhousie University, Halifax, Canada*

[16]*Department of Biochemistry and Robert-Cedergren Centre for Bioinformatics and Genomics, Université de Montréal, Montreal, Canada*

[17]*Institute of Cell Biology, University of Bern, Bern, Switzerland*

[18]*Center for Tropical and Emerging Global Diseases, University of Georgia, Athens, USA*

[19]*School of Marine and Atmospheric Sciences, Stony Brook University, Stony Brook, USA*

[20]*Department of Botany, University of British Columbia, Vancouver, Canada*

[21]*University of Delaware College of Earth, Ocean and Environment, Lewes, USA*

[22]*Woods Hole Oceanographic Institution, Woods Hole, MA, USA*

[23]*Facultad Ciencias Biológicas, Pontificia Universidad Católica de Chile, Fondo de Desarrollo de Areas Prioritarias, Center for Genome Regulation and Millennium Institute for Integrative Biology (iBio), Santiago de Chile, Chile*

[24]*School of Biosciences, University of Kent, Canterbury, Kent, UK*

[25]*Laboratory of Molecular and Evolutionary Parasitology, University of Kent, UK*

[26]*Graduate School of Life and Environmental Sciences, University of Tsukuba, Ibaraki, Japan*

[27]*Department of Mechanical Engineering, Massachusetts Institute of Technology, Boston, USA*

[28]*Department of Organismic and Evolutionary Biology, Harvard University, Cambridge, USA*

[29]*Centre for Organismal Studies, University of Heidelberg, Heidelberg, Germany*

[30]*Department of Parasitology, Faculty of Science, Charles University, BIOCEV, Vestec, Czech Republic*

[31]*Faculty of Life and Environmental Sciences, University of Tsukuba, Ibaraki, Japan*

[32]*School of Environmental Sciences, University of East Anglia, Norwich, UK*

[33]*Graduate School of Life Sciences, Tohoku University, Sendai, Miyagi, Japan*

[34]*Division of Environmental Photobiology, National Institute for Basic Biology, Okazaki, Aichi, Japan*

[35]*Department of Marine Sciences, University of Connecticut, Groton, USA*

[36]*School of Biosciences and Veterinary Medicine, University of Camerino, Camerino, Italy*

[37]*Department of Basic Biology, School of Life Science, Graduate University for Advanced Studies, Okazaki, Aichi, Japan*

[38]*Instituto de Biología Molecular y Celular de Rosario, CONICET, and Facultad de Ciencias Bioquímicas y Farmacéuticas, Universidad Nacional de Rosario, Rosario, Argentina*

[39]*Center for Genomics and Systems Biology, New York University, New York, USA*

[40]*Biological and Environmental Science and Engineering Division, King Abdullah University of Science and Technology, Thuwal, Jeddah, Saudi Arabia*

[41]*Center for Zoonosis Control, Global Institution for Collaborative Research and Education, Hokkaido University, Sapporo, Japan*

[42]*Department of Ecology and Evolution, Stony Brook University, Stony Brook, USA*

[43]*Lasry Center for Biosciences, Clark University, Worcester, USA*

[44]*Departament de Genètica Microbiologia i Estadística, Universitat de Barcelona, Barcelona, Catalonia, Spain*

[45]*Catalan Institution for Research and Advanced Studies, Barcelona, Catalonia, Spain*

[46]*Department of Systems Biology, Harvard Medical School, Boston, USA*

[47]*Wyss Institute for Biologically Inspired Engineering, Harvard University, Boston, USA*

[48]*Department of Environmental Biotechnology, Moss Landing Marine Laboratoriess, Moss Landing, USA*

[49]*Department of Molecular Genetics and Cell Biology, University of Chicago, Chicago, USA*

[50]*Department of Biology, California Institute of Technology, Pasadena, USA*

[51]*Instituto Milenio de Oceanografia de Chile, Concepción, Chile*

[52]*Institute of Oceanography, Minjiang University, Fuzhou, China*

[53]*Ocean EcoSystems Biology Unit, Marine Ecology Division, Helmholtz Centre for Ocean Research, Kiel, Germany*

[$]Present address: *AGADA Biosciences Inc., Halifax, Canada*

[**]Present address: *Institute de Biologie de l'ENS, Département de biologie, École Normale Supérieure, CNRS, INSERM, Paris, France*

[***]Present address: *Department of Microbiome Science, Max Planck Institute for Developmental Biology, Tübingen, Germany*

[&]Present address: *Max Planck Institute of Developmental Biology, Tubingen, Germany*

ABSTRACT

Marine microbial eukaryotes underpin the largest food web on the planet and influence global biogeochemical cycles that maintain habitability. They are also remarkably diverse and provide insights into evolution, including the origins of complex life forms, as revealed

126 through genome analyses. However, their genetic tractability has been limited to a few
127 species that do not represent the broader diversity of eukaryotic life or some of the most
128 environmentally relevant taxa. Here, we report on genetic systems developed as a community
129 resource for experimental cell biology of aquatic protists from across the eukaryotic tree and
130 primarily from marine habitats. We present evidence for foreign DNA delivery and
131 expression in 14 species never before transformed, report on the advancement of genetic
132 systems in 7 species, review of an already published transformation protocol in 1 species and
133 discuss why the transformation of 17 additional species has not been achieved yet. For all
134 protists studied in this community effort, we outline our methods, constructs, and genome-
135 editing approaches in the context of published systems. The reported breakthroughs on
136 genetic manipulation position the community to dissect cellular mechanisms from a breadth
137 of protists, which will collectively provide insights into ancestral eukaryotic lifeforms,
138 protein diversification and evolution of cellular pathways.
139

140 **INTRODUCTION**

141 The ocean represents the largest continuous planetary ecosystem, hosting an enormous
142 variety of organisms. These range from some of the largest creatures on Earth to a vast
143 microscopic biota including unicellular eukaryotes (protists). Despite their small size, protists
144 play key roles in marine biogeochemical cycles and harbor tremendous evolutionary
145 diversity[1-3]. Notwithstanding their significance for understanding the evolution of life on
146 Earth and their role in marine food webs, as well as driving biogeochemical cycles to
147 maintain habitability, little is known about their cell biology including reproduction,
148 metabolism, and signalling[4]. Most of the biological information available is based on
149 comparison of proteins from cultured genome-sequenced species to homologs in genetically
150 tractable model taxa, such as yeast[5-9]. A major impediment to understanding the cell biology

151 of these diverse eukaryotes is that protocols for genetic modification are only available for a
152 small number of species that represent neither the most ecologically relevant protists nor the
153 breadth of eukaryotic diversity.

154 The development of genetic tools requires reliable information about gene
155 organization and regulation of the emergent model species. Over the last decade, some of this
156 information has become available through genome[5,6,8,10] and transcriptome sequencing
157 initiatives[7,9,11,12] resulting in nearly 120 million unigenes from protists[13]. Insights from these
158 studies have enabled the phylogenetically-informed approach[7] used for selecting and
159 developing key marine protists into model systems in the Environmental Model Systems
160 (EMS) Project presented herein. Forty-one scientific groups took part in the EMS Project, a
161 collaborative effort resulting in the development of genetic tools that significantly expand the
162 number of eukaryotic lineages, which can be manipulated, and which encompass multiple
163 ecologically important marine protists.

164 Here, we summarize detailed methodological achievements by this collaborative
165 effort and analyse results to provide a synthetic 'Transformation Roadmap' for creating new
166 microeukaryotic model systems. Although the organisms reported here are diverse, the paths
167 to overcome difficulties share similarities, highlighting the importance of building a well-
168 connected community to overcome technical challenges and accelerate the development of
169 genetic tools. The 14 emerging model species presented herein, and the collective set of
170 genetic tools from the overall collaborative project, will not only extend our knowledge of
171 cell biology, evolution and functional biodiversity, but also serve as platforms to advance
172 microbial biotechnology.

173

174 **RESULTS**

175 ***Overview of taxa in the EMS Initiative***

Taxa were selected from multiple eukaryotic supergroups[1,7] to maximize the potential to compare fundamental aspects of cellular biology and to evaluate the numerous unigenes with unknown functions found in marine protists **(Fig. 1)**. Prior to the EMS initiative, reproducible transformation of marine protists was limited to only a few species such as *Thalassiosira pseudonana*, *Phaeodactylum tricornutum*, and *Ostreococcus tauri* (**Suppl. Table 1**). The EMS initiative included 39 species, specifically, 6 Archaeplastids, 2 Haptophytes, 2 Rhizarians, 9 Stramenopiles, 12 Alveolates, 4 Discobans, and 4 Opisthokonts (**Fig. 1**). Most of these taxa were isolated from coastal habitats, the focus area of several major culture collections[7]. More than 50% of the selected species are considered photoautotrophs, with another 35% divided between heterotrophic osmotrophs and phagotrophs, the remainder being predatory mixotrophs. Almost 20% of the chosen species are symbionts and/or parasites of marine plants or animals, 5% are associated with detritus, and several are responsible for harmful algal blooms (**Suppl. Table 2**).

While some transformation systems for some protists have been developed in the past[17,18], the challenge for this initiative was to develop novel genetic tools for species which not only require different cultivation conditions but are also phenotypically extremely diverse. It should be noted that not all major lineages could be pursued. For example, amoebozoans did not feature in the initiative, in part because they tend to be most important in soils, at least based on current knowledge, and manipulation systems exist for members of this eukaryotic supergroup, in particular *Dictyostelium discoideum*[14]. Below we summarize the taxa interrogated and overall EMS initiative outcomes (**Fig. 1**), provide evidence and detailed protocols for 14 taxa, for which no transformation systems have been previously reported (Category A), and 7 taxa for which existing protocols[15,17,18,25,40,44,45,51] were advanced (Category B) (**Figs. 2 and 3; Table 1**). We also review an already published transformation protocol[56] in 1 species (Category C), and we discuss the unsuccessful

transformation of 17 additional taxa, covering important phylogenetic positions in the eukaryotic tree of life (**Fig. 1**). Finally, we synthesize our findings in a roadmap for the development of transformation systems in protists (**Fig. 4**).

Archaeplastids. Prasinophytes are important marine green algae distributed from polar to tropical regions. They form a sister group to chlorophyte algae, and together, these two groups branch adjacent to land plants, collectively comprising the Viridiplantae, which are part of the Archaeplastida[1,8] (**Fig. 1**). Genome sequences are available for the picoprasinophytes (<3 µm cell diameter) tested herein, specifically, *Micromonas commoda*, *Micromonas pusilla*, *Ostreococcus lucimarinus* and *Bathycoccus prasinos*. As part of the EMS initiative, we report on the first genetic systems for *Bathycoccus*, a scaled, non-motile genus, and *Micromonas*, a motile, naked genus with larger genomes than *Bathycoccus* and *Ostreococcus*[8]. We also report on the first genetic systems for *Tetraselmis striata* and *Ostreococcus lucimarinus*. The latter was transformed based on an adapted homologous recombination system for *Ostreococcus tauri*[19].

O. lucimarinus (RCC802) and *B. prasinos* (RCC4222) were transformed using protocols adapted from *O. tauri*[20]. Briefly, using electroporation for transfer of exogenous genes, *O. lucimarinus* was transformed using a DNA fragment encoding the *O. tauri* high-affinity phosphate transporter (HAPT) gene fused to a luciferase gene and a KanMX selection marker (**Table 1; Suppl. Table 3**), which resulted in transient luciferase expression 24 h after electroporation (**Table 1; Fig. 3a**). After 2 weeks of growth in low melting agarose plates containing G418 (1 mg/ml), 480 colonies were obtained, picked, and grown in artificial seawater with the antibiotic neomycin. Of these, 76 displayed luminescence ≥ 2.5 fold above background (80 Relative Luminescence Units, RLU), with widely variable levels (200 to

225 31020 RLU), likely reflecting either the site of integration and/or the number of integrated
226 genes (**Fig. 3a; Suppl. Fig. 1; Suppl. sheet 1**).

227 The *O. tauri* construct did not work in *B. prasinos*, while the use of the *B. prasinos*
228 histone H4 and high affinity phosphate transporter sequences in an otherwise identical
229 construct and conditions was successful. Although luciferase expression was not detected 24
230 h after electroporation, 48 G418-resistant colonies were obtained 2 weeks later, 20 being
231 luminescent when grown in liquid medium. Analysis of 14 resistant transformants revealed
232 that the luciferase sequence was integrated into the genome of 5 clones that were
233 luminescent, and one non-luminescent clone (**Fig. 3b; Suppl. sheet 1)**, suggesting that the
234 chromatin context at integration sites in the latter was not favourable to luciferase expression.

235 Although transformation methods successful for *Bathycoccus* and *Ostreococcus* failed
236 in *Micromonas*, Lonza nucleofection was successful with *M. commoda* (CCMP2709) (**Table**
237 **1; Fig. 3c**) using 2 codon-optimized plasmids, one encoding the luciferase gene (NanoLuc,
238 Promega) flanked by an exogenous promoter and terminator sequence from the 5′- and 3′-
239 untranslated regions (UTRs) of histone H3 in *M. polaris*[8], and the other encoding an eGFP
240 gene flanked by endogenous promoter and terminator sequences from the ribosomal protein
241 S9. Acclimated mid-exponential *M. commoda* cells grown in L1 medium at 21 ºC were spun
242 at 5000 x *g* for 10 min, the pellet was resuspended in Buffer SF (Lonza) premixed with
243 carrier DNA (pUC19) and the plasmid, and 3 x 10^7 cells were used per reaction. After
244 applying the EW-113 pulse, 100 µl of ice-cold recovery buffer (10 mM HEPES-KOH, pH
245 7.5; 530 mM sorbitol; 4.7% [w/v] PEG 8000) was added to each well and incubated for 5 min
246 at room temperature. Each reaction was then transferred into 2 ml L1, placed at 21 °C and
247 light was increased stepwise over 72 h. Sensitivities to antibiotics were established (**Suppl.**
248 **Table 3**). Constructs did not include a selectable marker, as we aimed to introduce and
249 express foreign DNA while developing conditions suitable for transfection that supported

robust growth in this cell wall-lacking protist (**Table 1**). Transformants revealed a significantly higher level of eGFP fluorescence than wild type cells, with 1.3% of the population showing fluorescence per cell 45-fold higher than both the non-transformed portion of the culture and the wild type cells (**Fig. 3c; Suppl. sheet 1**). Additionally, the RLU was 1500-times higher than controls when using the luciferase-bearing construct, such that multiple experiments with both plasmids confirmed expression of exogenous genes in *M. commoda*.

T. striata (KAS-836) has been successfully transformed using microprojectile bombardment (**Suppl. Fig. 2**). Two selectable marker genes were tested, consisting of a putative promoter and 5' UTR sequences from the *T. striata* actin gene and either the coding sequences of the *Streptoalloteichus hindustanus* bleomycin gene (conferring resistance to zeocin) or the *Streptomyces hygroscopicus* bar gene (conferring resistance to glufosinate) (**Table 1; Suppl. Fig. 2)**. The terminator sequence was obtained from the *T. striata* *g*lyceraldehyde-3-phosphate dehydrogenase gene. Linearized plasmids were coated on gold particles and introduced into *T. striata* cells by using the PDS-1000/He Particle Delivery System (BioRad). Transformants were successfully selected on half-strength f/2 (seawater-distilled water in a 1:1 volume ratio) agar plates containing either 150 μg/ml zeocin or 150 μg/ml glufosinate.

***Haptophytes* (incertae sedis).** Haptophytes are a group of photosynthetic protists that are abundant in marine environments and include the major calcifying lineage, the coccolithophores. Genome sequences are available for *Emiliania huxleyi*[6] and *Chrysochromulina tobin*[21], and there is one report of nuclear transformation of a calcifying coccolithophore species[22]. Here, as part of the EMS initiative, a stable nuclear transformation system was developed for *Isochrysis galbana*, a species that lacks coccoliths, but represents

an important feedstock for shellfish aquaculture[23]. However, transformation of *Emiliania huxleyi,* which is the most prominent and ecologically significant coccolithophore, has not been achieved yet[24].

I. galbana (CCMP1323) was transformed by biolistic bombardment with the pIgNAT vector, which contains nourseothricin *N*-acetyltransferase (NAT, for nourseothricin resistance) driven by the promoter and terminator of Hsp70 from *E. huxleyi* (CCMP1516). Twenty four hours after bombardment, cells were transferred to liquid f/2 medium at 50% salinity containing 80 µg/ml nourseothricin (NTC) and left to grow for 2-3 weeks to select for transformants (**Table 1**). The presence of NAT in NTC-resistant cells was verified by PCR and RT-PCR (**Fig. 3d, Suppl. Fig. 3)** and the sequence verified. To confirm NTC resistance was a stable phenotype, cells were sub-cultured every 2-4 weeks at progressively higher NTC concentrations (up to 150 µg/ml) in the above-mentioned media. Cells remained resistant to NTC for approximately 6 months, as confirmed by PCR screening to identify the presence of the NAT gene.

***Rhizarians*.** Rhizarians include diverse non-photosynthetic protists, as well as the photosynthetic chlorarachniophytes that acquired a plastid *via* secondary endosymbiosis of a green alga. Uniquely, they represent an intermediate stage of the endosymbiotic process, since their plastids still harbor a relict nucleus (nucleomorph)[5]. Here, we report on an advanced transformation protocol for the chlorarachniophyte *Amorphochlora (Lotharella) amoebiformis* for which low-efficiency transient transformation has previously been achieved using particle bombardment[25].

A. amoebiformis (CCMP2058) cells (1 x 10^7) were resuspended in 100 µl of Gene Pulse Electroporation Buffer (BioRad) with 20 to 50 µg of the reporter plasmid encoding eGFP-RubisCO fusion protein under the control of the native *rbcS1* promoter and subjected

to electroporation (**Table 1**). Cells were immediately transferred to fresh ESM medium and incubated for 24 h. Transformation efficiency was estimated by the fraction of cells expressing eGFP, resulting in 0.03-0.1% efficiency, as enumerated by microscopy, showing an efficiency up to 1,000-fold higher than the previous study[25] (**Table 1**). Stable transformants were generated by manual isolation using a micropipette, and a transformed line has maintained eGFP fluorescence for at least 10 months without antibiotic selection (**Fig. 2; Fig. 3e**).

Stramenopiles. Stramenopiles are a diverse lineage with many important photoautotrophic, mixotrophic and heterotrophic taxa. As the most studied class in this lineage, diatoms (Bacillariophyceae) were early targets[26,18] for the development of reverse genetics tool[24]. Diatoms are estimated to contribute approximately 20% of annual carbon fixation[27] and, like several other algal lineages, are used in bioengineering applications and biofuels[28]. The transformation protocol for the Antarctic diatom *Fragilariopsis cylindrus*[29] represents the first transformation system for a cold-adapted eukaryote. A first transformation protocol has also been developed for *Pseudo-nitzschia multiseries*, a toxin-producing diatom[30]. Here we also present work for non-diatom stramenopiles, including the first transformation protocol for the Eustigmatophyte *Nannochloropsis oceanica*, and an alternative protocol for the Labyrinthulomycete *Aurantiochytrium limacinum*[31], both of which are used for biotechnological applications. Furthermore, we report on advances for CRISPR/Cas-driven gene knockouts in *P. tricornutum*[15,16] and a more efficient bacterial conjugation system for *T. pseudonana*[15].

Microparticle bombardment was used on *F. cylindrus* (CCMP1102) which was grown, processed and maintained at 4 °C in 24 hours light. Exponential phase cells (5 x 10^7 cells) were harvested onto a 1.2 µm membrane filter (Millipore) which was then placed on an

1.5% agar Aquil plate for bombardment with beads coated with a plasmid containing zeocin resistance and eGFP, both controlled by an endogenous fucoxanthin chlorophyll *a/c* binding protein (FCP) promoter and terminator (**Table 1; Suppl. Table 3**)[32]. Transformation was performed using 0.7 µm tungsten particles and the biolistic particle delivery system PDS1000/He (BioRad). Rupture discs for 1,350 and 1,550 pounds per square inch (psi) gave the highest colony numbers (efficiencies of 20.7 colony forming units (cfu)/10^8 cells and 30 cfu/10^8 cells), respectively. Following bombardment, the filter was turned upside down and left to recover (24 h) on the plate, then cells were rinsed from the plate/filter and spread across five 0.8% agar Aquil plates with 100 µg/ml zeocin. Colonies appeared 3 to 5 weeks later. PCR on genomic DNA showed that 100% and 60% of colonies screened positive for the zeocin resistance and eGFP genes, respectively. Confirmed by FACS and microscopy, eGFP was localized to the cytosol and was distinguishable from plastid autofluorescence (**Fig. 2**). Additional confirmation by PCR and RT-PCR (**Fig. 3f**) revealed that the *ShBle* gene for zeocin resistance and the gene encoding eGFP were present in the genomes of transformants after multiple transfers (> 10) two years later, indicating long-term stability.

Bacterial conjugation methods were improved in *T. pseudonana* (CCMP1335) using the silaffin precursor TpSil3p (**Table 1**) as the target gene. TpSil3p was fused to eGFP flanked by an FCP promoter and terminator, cloned into a pTpPuc3 episomal backbone, and transformed into mobilization plasmid-containing EPI300 *E. coli* cells (Lucigen). The donor cells were grown in SOC medium at 37 °C until OD_{600} of 0.3–0.4, centrifuged and resuspended in 267 µl SOC medium. Next, 200 µl donor cells were mixed with 4 x 10^7 *T. pseudonana* cells, co-cultured on pre-dried 1% agar plates, dark incubated at 30 °C for 90 min, then at 18 °C in constant light for 4 h, followed by selection in 0.25% agar pour plates containing 100 µg/ml NTC. Colonies were observed after 2 weeks, inoculated into 300 µl L1 medium and supplemented with 200 µg/ml NTC to reduce the number of false positives.

Positive transformants were identified by colony PCR screening (**Suppl. Fig. 4**) and epifluorescence microscopy (**Fig. 2**).

The diatom *Pseudo-nitzschia multiseries* (15093C) and other members of this genus form buoyant linear chains with overlapping cell tips during active growth, and were unconducive to punctate colony formation on agar, where their growth is generally poor. To address this challenge, a low-gelation-temperature agarose seawater medium (LGTA) was developed to facilitate growth, antibiotic selection, and cell recovery. *P. multiseries* exhibited growth inhibition at relatively low concentrations under NTC, formaldehyde, and zeocin (**Suppl. Table 3**). Biolistic transformation of two other *Pseudo-nitzschia* species had been demonstrated at low efficiency[33]. To complement this approach and explore potentially higher efficiency methods for transformation with diatom episomal plasmids, we modified the existing conjugation-based method[15]. The published conjugation protocol was modified to enhance *P. multiseries* post-conjugation viability by reducing SOC content. An episomal version of the Pm_actP_egfp_actT expression cassette was transfected into *E. coli* EPI300+pTAMOB and used for conjugation (**Table 1**). After 48 h in L1 medium, cells were plated in LGTA and eGFP-positive cells were observed 7 days later (**Fig. 2**). PCR revealed the presence of plasmids in all eGFP positive colonies (**Suppl. Fig. 5**). Similarly, conjugation with the episome pPtPUC3 (bleomycin selection marker)-containing bacterial donors was followed under zeocin selection (200 μg/ml). After 7 days, only viable cells (based on bright chlorophyll fluorescence) contained the episome, as confirmed by PCR. Propagation of transformants after the first medium transfer (under selection) has so far been unsuccessful.

Stable transformation of *A. limacinum* (ATCC MYA-1381) was achieved by knock-in of a resistance cassette composed of the bleomycin-resistance gene (*ShBle*) driven by 1.3 kb promoter and 1.0 kb terminator regions of the endogenous glyceraldehyde-3-phosphate dehydrogenase gene carried in a pUC19-based plasmid (18GZG) along with the native 18S

375 rRNA gene, and by knock-in of a similar construct containing a yeGFP:shble fusion (**Suppl.**
376 **Fig. 6**). Approximately 1 x 10^8 cells were electroporated (**Suppl. Table 4**), adapting the
377 electroporation protocol used for *Schizochytrium*[34]. The highest transformation efficiency was
378 achieved using 1 µg of linearized 18GZG plasmid with 2 pulses, resulting in a time constant
379 of ~5 ms (**Table 1**). Expression of the fusion protein was confirmed by both the zeocin-
380 resistance phenotype and the detection of eGFP (**Fig. 2**). Six 18GZG transformants derived
381 from uncut and linearized plasmids were examined in detail. All maintained antibiotic
382 resistance throughout 13 serial transfers, first in selective, and subsequently in non-selective
383 media, and then again in selective medium. Integration of the plasmid into the genome was
384 confirmed by PCR as well as by Southern blots using a digoxigenin-labeled ShBle gene
385 probe, showing that 4 transformants had integrations by single homologous recombination,
386 while in 2 transformants, additional copies of the antibiotic resistance cassette were
387 integrated by non-homologous recombination elsewhere in the genome (**Suppl. Fig. 6**).
388 Electroporation of *N. oceanica* (CCMP1779) was optimized based on observation of
389 cells treated with fluorescein-conjugated 2000 kDa dextran and subsequent survival (**Table**
390 **1**). A sorbitol concentration of 800 mM and electroporation at between 5 and 9 kV/cm
391 resulted in highest cell recovery. These conditions were used during introduction of plasmids
392 containing the gene for the blue fluorescent reporter mTagBFP2 under control of the
393 cytomegalovirus (CMV), the cauliflower Mosaic Virus 35S, or the VCP1 promoter
394 previously described from *Nannochloropsis* sp.[35]. Transient expression of blue fluorescence
395 (compared to cells electroporated simultaneously under the same conditions but without
396 plasmid) appeared within 2 h, lasted for at least 24 h, and disappeared by 48 h in subsets of
397 cells electroporated with mTagBFP2 under the control of CMV (**Suppl. Fig. 7).** The transient
398 transformation was more effective when a linearized plasmid was used compared to a circular

399 plasmid (**Table 1**). VCP1 did not induce blue fluorescence with a circular plasmid, while 35S
400 gave inconsistent results with either circularized or linearized plasmids.
401 For *P. tricornutum* (CCAP1055/1), we adapted the CRISPR/Cas9 system[16] for
402 multiplexed targeted mutagenesis. Bacterial conjugation[15] was used to deliver an episome
403 that contained a Cas9 cassette and 2 single-guide RNA (sgRNA) expression cassettes
404 designed to excise a 38-bp domain from the coding region of a nuclear-encoded, chloroplastic
405 glutamate synthase (Phatr3_J24739) and introduce an in-frame stop codon after strand
406 ligation (**Table 1**). The GoldenGate assembly was used to clone 2 expression cassettes
407 carrying sgRNAs into a *P. tricornutum* episome that contained a Cas9-2A-ShBle expression
408 cassette and the centromeric region CenArsHis (**Suppl. Fig. 8**). After their addition to a *P.*
409 *tricornutum* culture, plates were incubated in a growth chamber under standard growth
410 conditions for 2 days and transformed *P. tricornutum* colonies began to appear after 14 days.
411 Only colonies maintaining Cas9-2A-ShBle sequence on the delivered episome were able to
412 grow on selection plates because Cas9 and the antibiotic-resistant gene (ShBle) were
413 transcriptionally fused by the 2A peptide[36] (**Suppl. Fig. 8)**. Gel electrophoresis migration and
414 sequencing of the genomic target loci confirmed the 38-bp excision and premature stop
415 codon (**Fig. 3g**).
416
417 ***Alveolates.*** This species-rich and diverse group is comprised of ciliates, apicomplexans, and
418 dinoflagellates (**Fig. 1**). As a link between apicomplexan parasites and dinoflagellate algae,
419 perkinsids are key for understanding the evolution of parasitism, and also have potential
420 biomedical applications. Techniques currently exist for transformation of only a small
421 number of ciliates, perkinsids and apicomplexans[37,38]. Here, we present a first transformation
422 protocol for *Karlodinium veneficum* (CCMP1975), a mixotroph (combining photosynthetic
423 and phagotrophic nutrition) that produces fish-killing karlotoxins[39], and first evidence for

DNA delivery without gene expression in *Oxyrrhis marina* (CCMP 1788/CCMP 1795) and *Crypthecodinium cohnii* (CCMP 316), see **Suppl. Results, Table 1 and Supp. Fig. 17**) . Additionally, we report on improved transformation systems for *Perkinsus marinus* (PRA240) and *Amphidinium carterae* (CCMP1314) chloroplast, published recently as part of EMS initiative[40].

K. veneficum (CCMP1975) was transformed based on electroporation and cloning the selectable marker gene aminoglycoside 3'-phosphotransferase (*nptII / neo*; note that *nptII / neo* is used synonymously with amino 3'-glycosyl phosphotransferase gene (*aph(3')*) conferring resistance to kanamycin, neomycin, paromomycin, ribostamycin, butirosin and gentamicin B) into the backbone of the dinoflagellate-specific expression vector DinoIII-neo[41], which confers resistance to neomycin and kanamycin (**Table 1**). In brief, DinoIII-neo was linearized and electroporated using Nucleofector (Lonza). The preprogrammed Nucleofector optimization pulse codes, buffer SF/Solution I (Lonza), and 2 μg/μl of linearized DinoIII-neo were used. Electroporated cells were selected under 150 μg/ml kanamycin 3 days post-electroporation. Fresh seawater with kanamycin was added every 2 weeks to the cultures and new subcultures were inoculated monthly. After three months, DNA and RNA were isolated from the resistant cultures as previously reported[42,43] and cDNA was synthesized using random hexamers. Out of 16 transformations, two cell lines (CA-137, DS-138) showed stable growth under kanamycin selection. CA-137 developed dense cultures after 3 months, and the resistance gene was detected in both DNA and RNA through nested PCRs and RT-PCRs, respectively (**Suppl. Fig. 9, Fig. 3h**).

We improved the transformation protocol[44,45] of *Perkinsus marinus*, a pathogen of marine mollusks, fish, and amphibians[46], based on adapting the *A. carterae* transformation system[47]. In brief, a newly formulated transformation 3R buffer (200 mM Na_2HPO_4; 70 mM NaH_2PO_4; 15 mM KCl; 1.5 mM $CaCl_2$; 150 mM HEPES-KOH, pH 7.3) was used to reduce

449 the cost of electroporation. We co-expressed 2 genes and efficiently selected transient and
450 stable transformants using FACS (**Figs. 2 and 3i, Suppl. Fig. 10, Table 1**). In addition, we
451 established the integration profile of ectopic DNA once introduced into the *P. marinus*
452 genome. We did not see evidence of integration through homologous recombination and
453 observed a propensity for plasmid fragmentation and integration within transposable elements
454 sites. An optimized alternative protocol for transformation using glass bead abrasion was also
455 developed. In brief, 5 x 10^7 cells were resuspended in 330 µl of fresh ATCC Medium 1886
456 and were mixed with 5.0 µg of linearized and circular [1:1] plasmid and 300 µl of glass beads
457 (Sigma) in a 1.5 ml tube, vortexed for 30 s at maximum speed, and cells in 500 µl of culture
458 medium were transferred to 6-well plates in a final volume of 3 ml. Two versions of the
459 previously published Moe gene promoter were tested[44]. Whereas the 1.0 kb promoter version
460 induced expression after 2 or 3 days, the truncated version (0.5 kb) took 7 days for expression
461 to be detected. Resistance genes to bleomycin, blasticidin and puromycin have all been
462 shown to confer resistence to transformed *P. marinus*; however, selection regimes are still
463 relatively slow and inefficient, indicating further room for improvement[45].

464 We also report a new vector for the transformation of the *A. carterae* chloroplast, a
465 core, photosynthetic dinoflagellate. *A. carterae*, like other dinoflagellates with a peridinin-
466 containing chloroplast, contains a fragmented chloroplast genome made up of multiple
467 plasmid-like minicircles. The previous transformation protocols made use of this, to
468 introduce two vectors based on the *psbA* minicircle[40]. Here, we show that other minicircles
469 are also suitable for use as vectors. We created a new artificial minicircle, using the *atpB*
470 minicircle as a backbone, but replacing the *atpB* gene with a codon-optimized
471 chloramphenicol acetyl transferase. This circular vector was introduced by biolistics to *A.*
472 *carterae* (**Suppl. Fig. 11)**. Following selection with chloramphenicol, we were able to detect
473 transcription of the chloramphenicol acetyl transferase gene via RT-PCR (**Fig. 3j)**. This result

474 suggests that all of the 20 or so minicircles in the dinoflagellate chloroplast genome would be
475 suitable for use as artificial minicircles, thus providing a large pool of potential vectors.
476 For *O. marina,* a basal-branching phagotroph that lacks photosynthetic plastids and *C.*
477 *cohnii,* a heterotroph used in food supplements, we achieved DNA delivery (**Table 1, Suppl.**
478 **Fig. 17**) but not the expression of the delivered genes yet.
479
480 ***Discobans.*** This diverse group, recently split into Discoba and Metamonada[48], includes
481 heterotrophs, photoautotrophs, predatory mixotrophs, as well parasites. Discobans include
482 parasitic kinetoplastids with clinical significance, such as *Trypanosoma brucei*, *T. cruzi* and
483 *Leishmania* spp., for which efficient transformation protocols are available[49]. However, such
484 protocols are missing for aquatic species. Here, we describe the first available transformation
485 protocols for the kinetoplastid *Bodo saltans* and the heterolobosean *Naegleria gruberi*. The
486 former was isolated from a lake, but identical 18S rRNA sequence have been reported from
487 the marine environment[50]. The latter is a fresh water protist that represents a model organism
488 for closely related marine heterolobosean amoebas. Furthermore, we provide advanced
489 methods that build on published EMS results[51] for the diplonemid *Diplonema papillatum*.
490 *B. saltans* (ATCC 30904) was transformed with a plasmid containing a cassette
491 designed to fuse an endogenous EF-1α gene with eGFP for C-terminal tagging. This cassette
492 includes downstream of the eGFP, a *B. saltans* tubulin intergenic region followed by the
493 selectable marker gene *nptII / neo*, conferring resistance to neomycin. EF-1α genes exist in
494 tandem repeats. The homologous regions that flank the cassette were chosen as targets for
495 inducing homology-directed repair, however they target only one copy of the gene. As
496 transcription in *B. saltans* is polycistronic[52], insertion of the tubulin intergenic region into the
497 plasmid is essential for polyadenylation of the EF1-α/GFP fusion and *trans*-splicing of the
498 *nptII / neo* gene. Square-wave electroporation (Nepa21) was used with a poring pulse of

499 250V (25 ms) and 5 transfer pulses of 60V (99 ms) in the presence of Cytomix buffer (120
500 mM KCl; 0.15 mM $CaCl_2$; 10 mM KH_2PO_4; 2 mM EGTA; 5 mM $MgCl_2$; 25 mM HEPES-
501 KOH, pH 7.6). Selection of transfected cells began with 2 µg/ml of neomycin added 24 h
502 after electroporation, and this concentration was gradually increased over 2 weeks to 5 µg/ml
503 (**Table 1**). Cells were washed and subcultured into fresh selection medium every 4 days, and
504 neomycin-resistant cells emerged 7 to 9 days post-electroporation. The eGFP signal was
505 detected 2 days post-electroporation, albeit with low intensity. This may be due to the
506 inefficient translation of eGFP since it has not been codon-optimized for *B. saltans* (**Fig. 2**).
507 Genotyping analysis 9 months post-transfection confirmed the presence of the *nptII / neo*
508 gene and at least partial plasmid sequence (**Fig. 3k; Suppl. Fig. 12**). However, plasmid
509 integration into the *B. saltans* genome through homologous recombination is still
510 unconfirmed. This suggests either off-target plasmid integration or that the plasmid is
511 maintained episomally.

512 For *N. gruberi* (ATCC 30224) two plasmids were designed. The first one carried the
513 hygromycin B resistance gene (*hph*) with an actin promoter and terminator, along with an
514 HA-tagged eGFP driven by the ubiquitin promoter and terminator. The second plasmid
515 carried the *nptII / neo* gene instead. For each individual circular plasmid, 4 µg was
516 electroporated (**Table 1**). About 48 h after electroporation, dead cells were removed from the
517 suspension and viable cells were washed with PBS. Afterwards, 300 µg/ml of hygromycin B
518 or 700 µg/ml of neomycin was added to the fresh media. One to 4 weeks later, several
519 resistant clones were recovered and expression of eGFP and/or hygromycin was confirmed
520 by Western blotting (**Suppl. Fig. 13**). Expression of eGFP was observed by epifluorescence
521 microscopy (**Fig. 2; Suppl. Fig. 13**) with ~80% of transformants maintaining hygromycin B
522 or neomycin resistance in addition to expressing eGFP.

D. papillatum (ATCC 50162) was transformed by electroporation using 3 µg of *SwaI*-linearised fragment (cut from p57-V5+NeoR plasmid) containing V5-tagged *nptII / neo* gene flanked by partial regulatory sequences derived from the hexokinase gene of the kinetoplastid *Blastocrithidia* (strain p57) (**Table 1**) using a published protocol[51]. About 18 h after electroporation, 75 µg/ml G418 was added to the medium and after 2 weeks 7 neomycin-resistant clones were recovered. Transcription of *nptII / neo* was verified in 4 clones by RT-PCR **(Suppl. Fig. 14)** and the expression of the tagged *nptII / neo* protein was confirmed in 2 clones by Western blotting using α-V5 antibody (**Fig. 4l**).

Opisthokonts

The opisthokont clade Holozoa includes animals and their closest unicellular relatives Choanoflagellates, Filastereans, Ichthyosporeans, and Corallochytreans. The establishment of genetic tools in non-metazoan holozoans promises to help illuminate the cellular and genetic foundations of animal multicellularity[9]. Genomic and transcriptomic data are available for multiple representatives characterized by diverse cell morphologies, some of which can even form multicellular structures[9,12]. Untill recently, only transient transformations have been achieved for some opistokonts such as the filasterean *Capsaspora owczarzaki*[53], the ichthyosporean *Creolimax fragrantissima*[54] and the choanoflagellate *Salpingoeca rosetta*[55]. Through the EMS initiative, we report on the first evidence for transient transformation of the ichthyosporean *Abeoforma whisleri*, isolated from the digestive tract of mussels, and review on recently published stable transformation protocol for *S. rosetta* achieved by using the selectable marker gene (puromycin N-acetyl-transferase - *PAC*) (**Fig. 2**)[56].

All *A. whisleri* life stages are highly sensitive to a variety of methods for transformation. However, we developed a Lonza 4D-nucleofection-based protocol using 16-well strips, wherein PBS-washed cells were resuspended in 20 µl of buffer P3 (Lonza)

548 containing 40 μg of carrier plasmid (empty pUC19) and 1-5 μg of the reporter plasmid (*A.*
549 *whisleri* H2B fused to mVenus fluorescent protein, mVFP) (**Table 1**), and subjected to code
550 EN-138 (Lonza). Immediately after the pulse, cells were recovered by adding 80 μl of marine
551 broth (Gibco) prior to plating in 12-well culture plates previously filled with 1 ml marine
552 broth. After 24 h, ~1% of the culture was transformed based on the fraction of cells
553 expressing mVFP in the nucleus (**Figs. 2 and 3m**).

554 ***Microbial eukaryotes in natural planktonic communities***

555 Model organisms are typically selected based on criteria, such as relative ease of isolation
556 and asexual cultivation in the laboratory. These attributes may not correlate with the capacity
557 for uptake and expression of the exogenous DNA, so we explored whether such propensity
558 was common or rare in natural marine planktonic pico- and nanoeukaryote communities in a
559 culture-independent manner. Microbial plankton from natural seawater was concentrated and
560 electroporated with the plasmids containing mTagBFP2 under the control of CMV or 35S
561 promoters (see **Suppl. Results**). In most trials, blue fluorescent cells were very rare if
562 detected at all (compared to control samples). However, in one natural community tested a
563 particular picophytoeukaryote population was present where up to 50% transiently expressed
564 blue fluorescence when the CMV promoter was used (**Suppl. Fig. 15**). This suggests it might
565 be possible to selectively culture eukaryotic microorganisms based on capacity to express
566 exogenous DNA.
567
568 **Discussion**
569 Marine organisms play essential roles in global biogeochemical cycles and produce
570 approximately half of the Earth's oxygen[1,27]. Decades of research by marine biologists,
571 ecologists, protistologists, and oceanographers have contributed to an increasingly coherent

572 picture of the oceanic ecosystem. These studies highlight the diversity of ocean life, including
573 the protistan component[2,3]. Remarkable strides have also been made in developing an
574 overview of the genomes and predicted proteomes of these protists[13]. However, without
575 genetic manipulation systems, these taxa have remained an untapped resource for providing
576 deeper insights into their cell biology, with potentially valuable outcomes for evolutionary
577 studies, nanotechnology, biotechnology, medicine, and pharmacology.

578 The results of the EMS initiative were enhanced by the research teams having met and
579 conversed over a 3-year period. This facilitated identification and optimization of the steps
580 required to create new model systems in aquatic protists, ultimately culminating in our
581 roadmap for establishing new model organisms (**Fig. 4**). Successes and failures with
582 selectable markers, transformation conditions, and reporters were qualitatively compared
583 across species (**Suppl. Tables 3, 4 and 5**), and efforts were detailed using consistent
584 terminology (**Table 1; Figs. 2 and 3**). An important aspect of establishing a roadmap is to
585 also incorporate information on partially successful (e.g. DNA delivered) or failed
586 approaches as done herein (**Suppl. Results**).

587 For some of the selected species, the first step was to identify cultivation conditions
588 for robust growth in the laboratory to either generate high cell densities or large culture
589 volumes for obtaining sufficient biomass required for a variety of molecular biology
590 methods. Unlike established microbial model species, cultivation of marine protists can be
591 challenging especially under axenic conditions and for predatory taxa that require co-
592 cultivation with their prey. Nevertheless, 13 out of 35 species have been made axenic prior to
593 the development of transformation protocols. For the remaining species, we were unable to
594 remove bacteria and therefore had to make sure that the transformation signals were coming
595 from the targeted protist rather than contaminants (**Suppl. Table 2**). Subsequent steps
596 included the identification of suitable antibiotics and their corresponding selectable markers

(**Table 1; Suppl. Table 3**), conditions for introducing exogenous DNA (**Table 1; Suppl. Table 4**), and selection of promoter and terminator sequences for designing transformation vectors (**Table 1; Suppl. Table 5; Suppl. Doc. 1**).

As exemplified in the new systems provided herein (**Figs. 2 and 3; Table 1**), a variety of methods were used to test whether exogenous DNA was integrated into the genome or maintained as a plasmid, and whether the introduced genes were expressed. Approaches to show the former included inverse PCR, Southern blotting and whole genome sequencing, whereas approaches to demonstrate the latter included various combinations of PCR, RT-PCR, Western blotting, epifluorescence microscopy, fluorescence-activated cell sorting (FACS), antibody-based methods, and/or growth assays in the presence of antibiotics to confirm transcription and translation of introduced selection and reporter genes (e.g., eGFP, YFP, mCherry). For fluorescent markers, it was first ensured that the wild type, or manipulated controls cells, had no signals conflicting with the marker (e.g. **Fig. 2**, **Fig. 3C**), an important step because photosynthetic protists contain chlorophyll and other autofluorescent pigments. Overall transformation outcomes for each species were parsed into three groups according to the level of success or lack thereof (A = first transformation protocol for a given species; B = advanced protocol based on prior work; C = published protocol based on the EMS initiative) and are discussed below according to their phylogenetic position (**Fig. 1**).

Our studies did not result in a universally applicable protocol, likely because transformability and a range of other key conditions varied greatly across taxa and approaches. Factors influencing outcomes include intrinsic features of the genome (e.g., presence/absence of homologous recombination, extrachromosomal elements, genome size, level of ploidy), as well as morphology and structural features of the cell. In general, electroporation proved the most common method for introducing exogenous DNA stably into

the cell. This approach was utilized for naked cells and protoplasts, yet frequently also worked, albeit with lower efficiency, on cells protected by cell walls. Linearized plasmids were most effective for delivery, and 5' and 3' UTRs-containing promotors of highly expressed endogenous genes provided the strongest expression of selective reporters and markers. The collaborative network facilitated many of the studies undertaken in this initiative. The names and contact details of all co-authors assigned to particular species are listed in **Suppl. Table 6**. Lessons from our integrated approach for instance include examples such as the adoption of the highly sensitive reporter *nanoluc* (*Nluc*) gene by several teams for initial rapid screening to find optimal conditions for transformation. If successful, teams usually continued with fluorescence-based or other methods, as well as a hypertonic recovery buffer. Furthermore, large amounts of carrier DNA usually facilitated successful initial transformations (e.g. *M. commoda*, *A. whisleri*) or improved existing protocols (*S. rosetta*[55]).

As outlined above, the global synthesis of approaches developed, or failed, herein, and in published EMS studies provides a 'Transformation Roadmap' to guide future efforts to establish or improve new and emergent model organisms (**Fig. 4**). However, it also allows us to identify lineages that were particularly problematic – in that despite efforts of several teams, successful expression of foreign DNA, whether transient or stable, was not achieved. Here, dinoflagellates and the coccolithophore *E. huxleyi* were particularly recalcitrant to our efforts and often, even if it appeared that DNA was delivered (**Suppl. Table 5**), expression of encoded genes was not confirmed, and the number of transfected cells was very low. For example, in the case of *C. cohnii*, DNA appeared ultimately to be delivered using Lonza based approaches. However, after testing of multiple methods and plasmids (PmMOE:GFP-11, UB-GFP, EF-GFP, PAY and PAYCO) there were no positive outcomes. Furthermore, attempts to use the successful system developed for *A. carterae* for transforming its relative

646 *Symbiodinium microadriaticum* were unsuccessful[57]. These and other lineages such as
647 coccolithophores, warrant concerted future efforts.

648 The combination of new results presented herein and others arising from the EMS
649 initiative[58] significantly expand the segment of extant eukaryotic diversity amenable to
650 reverse genetics approaches. Out of the 39 microbial eukaryotes selected for the initiative,
651 exogenous DNA was delivered and expressed in more than 50% of them. This high rate of
652 success testifies to the benefits of taking on high-risk research in a large, open, and
653 collaborative context[58]. Moreover, the new systems reported herein open a wealth of
654 opportunities for exploring functional differences between members of relatively conserved
655 protein families shared across eukaryotes, or even domains of life. Collectively, these novel
656 and recently described protistan transformation systems enable us for the first time to shed
657 light on the function of species-specific genes which likely reflect key adaptations to specific
658 niches in dynamic ocean habitats.

659

660 **ACKNOWLEDGEMENTS**

661 We thank M. Salisbury and D. Lacono for assistance, C. Poirier and M. Hamilton (Monterey
662 Bay Aquarium Research Institute/GEOMAR) for FACS analysis; and V. K. Nagarajan, M.
663 Accerbi, and P. J. Green (University of Delaware) who carried out *Agrobacterium* studies in
664 *Heterosigma akashiwo*; and N. Kraeva, C. Bianchi and V. Yurchenko (University of Ostrava)
665 for the help with designing the p57-V5+NeoR construct. We are also grateful to the
666 protocols.io team for their support and thank four anonymous reviewers for their constructive
667 criticisms of our manuscript. This collaborative effort was supported by the Gordon and Betty
668 Moore Foundation EMS Program of the Marine Microbiology Initiative and other forms of
669 grant support to the participating laboratories.

670

AUTHOR CONTRIBUTIONS

The project was conceived and designed by A.C.J., J.Z.K., S.B., D.F., J.L., R.E.R.N., J.A.F.R., E.C., L.S., A.Z.W., T.M., A.E.A., F.Y.B, C.B, Ch.B., H.C., T.C., J.L.C., K.C., C.L.D., V.E., V.H., Y.H., C.J.H., P.J.K., N.K., S.L., C.M., J.M., I.R.T., P.A.S., C.H.S., G.J.S., A.T., P.V.D., A.T. and R.F.W. Data analysis was carried out by M.A.J., C.A., C.B., A.C.B., P.B., D.S.B., S.A.B., A.B., G.B., R.C., M.A.C., D.B.C., L.C., R.D., E.E., P.A.E., F.F., V.F.B., N.J.F., K.F., P.A.G., P.R.G., F.G., S.G., J.G., Y.H., E.R.H.C., E.H., A.Hi., A.Ho., I.H., J.I., N.A.T.I., Y.I., N.E.J., A.K., K.F.K., B.K., E.K., L.A.K., N.L., I.L., Z.L., J.C.L., F.L., S.M., T.M., M.M., S.R.N., D.N., I.C.N., L.N., A.M.G.N.V., M.N., I.N., A.Pa., A.Pi., S.P., J.P., J.S.R., M.R., D.R., A.R., M.A.S., E.S., B.S., R.S.,T.V.H., L.T., J.T., M.V., V.V., L.W., X.W., G.W., A.W. and H.Z. The manuscript was written by D.F., R.E.R.N., J.A.F.R., E.C., L.S., T.M., A.Z.W. and J.L. with input from all authors.

COMPETING INTERESTS

The authors declare no competing interests.

REFERENCES

1. Worden, A. Z., Follows, M. J., Giovannoni, S. J., Wilken, S., Zimmerman, A. E. & Keeling, P. J. Rethinking the marine carbon cycle: Factoring in the multifarious lifestyles of microbes. *Science* **347**, 1257594 (2015).

2. de Vargas, C., Audic, S., Henry, N., Decelle, J., Mahé, F., Logares, R., Lara, E., Berney, C., Le Bescot, N., Probert, I., Carmichael, M., Poulain, J., Romac, S., Colin, S., Aury, J. M., Bittner, L., Chaffron, S., Dunthorn, M., Engelen, S., Flegontova, O., Guidi, L., Horák, A., Jaillon, O., Lima-Mendez, G., Lukeš, J., Malviya, S., Morard, R., Mulot, M., Scalco, E., Siano, R., Vincent, F., Zingone, A., Dimier, C., Picheral, M., Searson, S., Kandels-

Lewis, S., Tara Oceans Coordinators., Acinas, S. G., Bork, P., Bowler, C., Gorsky, G., Grimsley, N., Hingamp, P., Iudicone, D., Not, F., Ogata, H., Pesant, S., Raes, J., Sieracki, M. E., Speich, S., Stemmann, L., Sunagawa, S., Weissenbach, J., Wincker, P. & Karsenti, E. Eukaryotic plankton diversity in the sunlit global ocean. *Science* **348**, 1261605 (2015).

3. Duarte, C. M., Regaudie-de-Gioux, A., Arrieta, J. M., Delgado-Huertas, A. & Agustí, S. The oligotrophic ocean is heterotrophic. *Annu. Rev. Mar. Sci.* **5**, 551-569 (2013).

4. Collier, J. L. & Rest, J. S. Swimming, gliding, and rolling toward the mainstream: cell biology of marine protists. *Mol. Biol. Cell.* **30**, 1245-1248 (2019).

5. Curtis, B. A., Tanifuji, G. & Burki, F. Algal genomes reveal evolutionary mosaicism and the fate of nucleomorphs. *Nature* **492**, 59–65 (2012).

6. Read, B. A., Kegel, J., Klute, M. J., Kuo, A., Lefebvre, S. C., Maumus, F., Mayer, C., Miller, J., Monier, A., Salamov, A., Young, J., Aguilar, M., Claverie, J. M., Frickenhaus, S., Gonzalez, K., Herman, E. K., Lin, Y. C., Napier, J., Ogata, H., Sarno, A. F., Shmutz, J., Schroeder, D., de Vargas, C., Verret, F., von Dassow, P., Valentin, K., Van de Peer, Y., Wheeler, G., *Emiliania huxleyi* Annotation Consortium, Dacks, J. B., Delwiche, C. F., Dyhrman, S. T., Glöckner, G., John, U., Richards, T., Worden, A. Z, Zhang, X. & Grigoriev, IV. Pan genome of the phytoplankton *Emiliania* underpins its global distribution. *Nature* **499**, 209-213 (2013).

7. Keeling P. J., Burki, F., Wilcox, H. M., Allam, B. & Allen, E. E. The Marine Microbial Eukaryote Transcriptome Sequencing Project (MMETSP): illuminating the functional diversity of eukaryotic life in the oceans through transcriptome sequencing. *PLoS Biol*. **12**, e1001889 (2014).

8. van Baren, M. J., Bachy, C., Reistetter, E. N., Purvine, S. O., Grimwood, J., Sudek, S., Yu, H., Poirier, C., Deerinck, T. J., Kuo, A., Grigoriev, IV., Wong, C. H., Smith, R. D., Callister, S. J., Wei, C. L., Schmutz, J. & Worden, A. Z. Evidence-based green algal genomics reveals marine diversity and ancestral characteristics of land plants. *BMC Genomics* **17**, 1–22 (2016).

9. Richter, D. J., Fozouni, P., Eisen, M. & King, N. Gene family innovation, conservation and loss on the animal stem lineage. *eLife* **7**, 1–43 (2018).

10. Strassert, J. F. H., Karnkowska, A., Hehenberger, E., Del Campo, J., Kolisko, M., Okamoto, N., Burki, F., Janouškovec, J., Poirier, C., Leonard, G., Hallam, S. J., Richards, T. A., Worden, A. Z., Santoro, A. E. & Keeling, P. J. Single cell genomics of uncultured marine alveolates shows paraphyly of basal dinoflagellates. *ISME J.* **12**, 304-308 (2018).

11. Joseph, S. J., Fernández-Robledo, J. A., Gardner, M. J., El-Sayed, N. M., Kuo, C. H., Schott, E. J.,Wang, H., Kissinger, J. C. & Vasta, G. R. The Alveolate *Perkinsus marinus*: Biological insights from EST gene discovery. *BMC Genomics* **11**, 228 (2010).

12. Grau-Bové, X., Torruella, G., Donachie, S., Suga, H., Leonard, G., Richards, T. A. & Ruiz-Trillo, I. Dynamics of genomic innovation in the unicellular ancestry of animals. *eLife* **6**, e26036 (2017).

13. Carradec, Q., Pelletier, E., Da Silva, C., Alberti, A. & Seeleuthner, Y. A global atlas of eukaryotic genes. *Nat. Commun.* **9**, 373 (2018).

14. Paschke, P., Knecht, D. A., Williams, T. D., Thomason, P. A., Insall, R. H., Chubb, J. R., Kay, R. R. & Veltman, D. M. Genetic engineering of *Dictyostelium discoideum* cells based on selection and growth on bacteria. *J. Vis. Exp.* **143**, e58981 (2019).

15. Karas, B. J., Diner, R. E., Lefebvre, S. C., McQuaid, J., Phillips, A. P., Noddings, C. M., Brunson, J. K., Valas, R. E., Deerinck, T. J., Jablanovic, J., Gillard, J. T., Beeri, K., Ellisman, M. H., Glass, J. I., Hutchison, C. A. 3rd., Smith, H. O., Venter, J. C., Allen, A. E., Dupont, C. L. & Weyman, P. D. Designer diatom episomes delivered by bacterial conjugation. *Nat. Commun.* **6**, 6925 (2015).

16. Nymark, M., Sharma, A. K., Sparstad, T., Bones, A. M. & Winge, P. A. CRISPR/Cas9 system adapted for gene editing in marine algae. *Sci. Rep.* **6**, 24951 (2016).

17. Hopes, A., Nekrasov, V., Kamoun, S. & Mock, T. Editing of the urease gene by CRISPR-Cas in the diatom *Thalassiosira pseudonana*. *Plant Methods* **12**, 49 (2016).

18. Apt, K. E., Kroth-Pancic, P. G. & Grossman, A. R. Stable nuclear transformation of the diatom *Phaeodactylum tricornutum*. *Mol. Gen. Genet*. **252**, 572-579 (1996).

19. Lozano, J. C., Schatt, P., Botebol, H., Vergé, V., Lesuisse, E., Blain, S., Carré, I. A. & Bouget, F. Y. Efficient gene targeting and removal of foreign DNA by homologous recombination in the picoeukaryote *Ostreococcus*. *Plant J*. **78**, 1073-1083 (2014).

20. Van Ooijen, G., Knox, K., Kis, K., Bouget, F. Y. & Millar, A. J. Genomic transformation of the picoeukaryote *Ostreococcus tauri*. *J. Vis. Exp*. **65**, e4074 (2012).

21. Hovde, B. T., Deodato, C. R., Hunsperger, H. M., Ryken, S. A., Yost, W., Jha, R. K., Patterson, J., Monnat, R. J. Jr., Barlow, S. B., Starkenburg, S. R. & Cattolico, R. A. Genome sequence and transcriptome analyses of *Chrysochromulina tobin*: Metabolic tools for enhanced algal fitness in the prominent order Prymnesiales (Haptophyceae). *PLoS Genet*. **11**, e1005469 (2015).

763 22. Endo, H., Yoshida, M., Uji, T., Saga, N., Inoue, K. & Nagasawa, H. Stable nuclear
764 transformation system for the coccolithophorid alga *Pleurochrysis carterae*. *Sci. Rep.* **6**,
765 22252 (2016).

766 23. Dörner, J., Carbonell, P., Pino, S. & Farias, A. Variation of fatty acids in *Isochrysis*
767 *galbana* (T-Iso) and *Tetraselmis suecica*, cultured under different nitrate availabilities. *J.*
768 *Fish. Aquacult.* **5**, 1-3 (2014).

769 24. Velmurugan, N. & Deka, D. Transformation techniques for metabolic engineering of
770 diatoms and haptophytes: current state and prospects. *Appl Microbiol Biotechnol.* **102**,
771 4255-4267 (2018).

772 25. Hirakawa, Y., Kofuji, R. & Ishida, K. Transient transformation of a chlorarachniophyte
773 alga, *Lotharella amoebiformis* (chlorarachniophyceae), with uidA and egfp reporter genes.
774 *J. Phycol*. **44**, 814–20 (2008).

775 26. Dunahay, T. G., Jarvis, E. E. & Roessler, P. G. Genetic transformation of the diatoms
776 *Cyclotella cryptica* and *Navicula saprophila. J. Phycol.* **31**, 1004–1012 (1995).

777 27. Field, C. B., Behrenfeld, M. J., Randerson, J. T. & Falkowski, P. Primary production of
778 the biosphere: Integrating terrestrial and oceanic components. *Science* **281**, 237-240
779 (1998).

780 28. Mishra, M., Arukha, A. P., Bashir, T., Yadav, D. & Prasad, G. B. K. S. All new faces of
781 diatoms: Potential source of nanomaterials and beyond. *Front. Microbiol.* **8**, 1239 (2017).

782 29. Mock, T., Otillar, R. P., Strauss, J., McMullan, M., Paajanen, P., Schmutz, J., Salamov, A.,
783 Sanges, R., Toseland, A., Ward, B. J., Allen, A. E., Dupont, C. L., Frickenhaus, S.,
784 Maumus, F., Veluchamy, A., Wu, T., Barry, K. W., Falciatore, A., Ferrante, M. I.,
785 Fortunato, A. E., Glöckner, G., Gruber, A., Hipkin, R., Janech, M. G., Kroth, P. G., Leese,

F., Lindquist, E. A., Lyon, B. R., Martin, J., Mayer, C., Parker, M., Quesneville, H., Raymond, J. A., Uhlig, C., Valas, R. E., Valentin, K. U., Worden, A. Z., Armbrust, E. V., Clark, M. D., Bowler, C., Green, B. R., Moulton, V., van Oosterhout, C. & Grigoriev, IV. Evolutionary genomics of the cold-adapted diatom *Fragilariopsis cylindrus*. *Nature* **541**, 536–540 (2017).

30. Brunson, J. K., McKinnie, S. M. K., Chekan, J. R., McCrow, J. P., Miles, Z. D., Bertrand, E. M., Bielinski, V. A., Luhavaya, H., Oborník, M., Smith, G. J., Hutchins D. A., Allen, A. E. & Moore, B. S. Biosynthesis of the neurotoxin domoic acid in a bloom-forming diatom. *Science* **361**, 1356-1358 (2018).

31. Sakaguchi K., Matsuda T., Kobayashi T., Ohara J., Hamaguchi R., Abe E., Nagano N., Hayashi M., Ueda M., Honda D., Okita Y., Taoka Y., Sugimoto S., Okino N. & Ito M. Versatile transformation system that is applicable to both multiple transgene expression and gene targeting for thraustochytrids. *Applied and Environmental Microbiology* **78**: 3193-3202 (2012).

32. Kroth, P. G. Genetic Transformation; A tool to study protein targeting in diatoms. *Methods Mol. Biol*. **390**, 257–267 (2007).

33. Sabatino, V., Russo, M. T., Patil, S., d'Ippolito, G., Fontana, A. & Ferrante, M. I. Establishment of genetic transformation in the sexually reproducing diatoms Pseudo-*nitzschia multistriata* and *Pseudo-nitzschia arenysensis* and inheritance of the transgene. *Marine Biotech.* **17**, 452-462 (2015).

34. Ono, K., Aki, T. & Kawamoto, S. Method for introducing a gene into labyrinthulomycota. US Patent 7,888,123 (2011).

35. Kilian, O., Benemann, C. S., Niyogi, K. K. & Vick, B. High-efficiency homologous recombination in the oil-producing alga *Nannochloropsis sp. Proc. Natl. Acad. Sci. USA* **108**, 21265-21269 (2011).

36. Duda, K., Lonowski, L. A., Kofoed-Nielsen, M., Ibarra, A., Delay, C. M., Kang, Q., Yang, Z., Pruett-Miller, S. M., Bennett, E. P., Wandall, H. H., Davis, G. D., Hansen, S. H. & Frödin, M. High-efficiency genome editing via 2A-coupled co-expression of fluorescent proteins and zinc finger nucleases of CRISPR/Cas9 nicase pairs. *Nucl. Acids. Res.* **42**, e84 (2014).

37. Donald, R. G. & Roos, D. S. Stable molecular transformation of *Toxoplasma gondii*: a selectable dihydrofolate reductase-thymidylate synthase marker based on drug-resistance mutations in malaria. *Proc. Natl. Acad. Sci. USA* **90**, 11703-11707 (1993).

38. Rug, M. & Maier, A. G. Transfection of *Plasmodium falciparum. Methods Mol. Biol.* **923**, 75-98 (2013).

39. Barbrook, A. C., Howe, C. & Nisbet, R. Breaking up is hard to do: the complexity of the dinoflagellate chloroplast genome. *Perspect. Phycol.* https://doi.org/10.1127/pip/2018/0084 (2018).

40. Nimmo, I. C., Barbrook, A. C., Chen, J. E., Geisler, K., Smith, A. G., Aranda, A., Purton, P., Waller, R. F., Nisbet, R. E. R. & Howe, C. J. Genetic transformation of the dinoflagellate chloroplast. *eLife* **8**, e45292 (2019).

41. Sprecher, B. N., Zhang, H. & Lin, S. Nuclear gene transformation in a dinoflagellate. *bioRxiv* 602821 (2019).

829 42. Zhang, H., Campbell, D. A., Sturm, N. R., Rosenblad, M. A., Dungan, C. F. & Lin, S.
830 Signal recognition particle RNA in dinoflagellates and the perkinsid *Perkinsus marinus*.
831 *Protist* **164**, 748-761 (2013).

832 43. Lin, S., Zhang, H. & Dubois, A. Low abundance distribution of Pfiesteria piscicida in
833 Pacific and Western Atlantic as detected by mtDNA-18S rDNA real-time polymerase
834 chain reaction. *J. Plankton Res*. **28**, 667-681 (2006).

835 44. Fernández Robledo, J. A., Lin, Z. & Vasta, G. R. Transfection of the protozoan parasite
836 *Perkinsus marinus. Mol. Biochem. Parasitol*. **157**, 44-53 (2008).

837 45. Sakamoto, H., Hirakawa, Y., Ishida, K. I., Keeling, P. J., Kita, K. & Matsuzaki M.
838 Puromycin selection for stable transfectants of the oyster-infecting parasite *Perkinsus*
839 *marinus. Parasitol. Int*. **69**, 13-16 (2018).

840 46. Chambouvet, A., Gower, D. J., Jirků, M., Yabsley, M. J., Davis, A. K., Leonard, G.,
841 Maguire, F., Doherty-Bone, T. M., Bittencourt-Silva, G. B., Wilkinson, M. & Richards,
842 T. A. Cryptic infection of a broad taxonomic and geographic diversity of tadpoles by
843 Perkinsea protists. *Proc. Natl. Acad. Sci. USA* **112**, E4743-4751 (2015).

844 47. Ten Lohuis, M. R. & Miller, D. J. Genetic transformation of dinoflagellates (*Amphidinium*
845 and *Symbiodinium*): expression of GUS in microalgae using heterologous promoter
846 constructs. *Plant J.* **13**, 427-435, (1998).

847 48. Adl, S. M., Bass, D., Lane, C. E., Lukeš, J., Schoch, C. L., Smirnov, A., Agatha, S., Berney,
848 C., Brown, M. W., Burki, F., Cárdenas, P., Čepička, I., Chistyakova, L., Del Campo, J.,
849 Dunthorn, M., Edvardsen, B., Eglit, Y., Guillou, L., Hampl, V., Heiss, A. A., Hoppenrath,
850 M., James, T. Y., Karnkowska, A., Karpov, S., Kim, E., Kolisko, M., Kudryavtsev, A.,
851 Lahr, D. J. G., Lara, E., LeGall, L., Lynn, D. H., Mann, D. G., Massana, R., Mitchell, E.

852 A. D., Morrow, C., Park, J. S., Pawlowski, J. W., Powell, M. J., Richter, D. J., Rueckert,
853 S., Shadwick, L., Shimano, S., Spiegel, F. W., Torruella, G., Youssef, N., Zlatogursky, V.
854 & Zhang, Q. Revision to the classification, nomenclature and diversity of eukaryotes. *J.*
855 *Euk. Microbiol*. **66**, 4-119 (2019).

856 49. Matthews, K. R. 25 years of African trypanosome research: From description to molecular
857 dissection and new drug discovery. *Mol. Biochem. Parasitol.* **200**, 30-40 (2015).

858 50. Jackson, A. P., Quail, M. A. & Berriman, M. Insights into the genome sequence of a free-
859 living Kinetoplastid: *Bodo saltans* (Kinetoplastida: Euglenozoa). *BMC Genomics* **9**, 594
860 (2008).

861 51. Kaur, B., Valach, M., Peña-Diaz, P., Moreira, S., Keeling, P. J., Burger, G., Lukeš, J. &
862 Faktorová, D. Transformation of *Diplonema papillatum*, the type species of the highly
863 diverse and abundant marine micro-eukaryotes Diplonemida (Euglenozoa). *Env.*
864 *Microbiol*. **20**, 1030-1040 (2018).

865 52. Opperdoes, F. R., Butenko, A., Flegontov, P., Yurchenko, V. & Lukeš, J. Comparative
866 metabolism of free-living *Bodo saltans* and parasitic trypanosomatids. *J. Eukaryot.*
867 *Microbiol*. **63**, 657-678 (2016).

868 53. Parra-Acero, H., Ros-Rocher, N., Perez-Posada, A., Kożyczkowska, A., Sánchez-Pons, N.,
869 Nakata, A., Suga, H., Najle, S. R. & Ruiz-Trillo, I. Transfection of *Capsaspora owczarzaki*,
870 a close unicellular relative of animals. *Development* **145**, 162107 (2018).

871 54. Suga, H. & Ruiz-Trillo, I. Development of ichthyosporean sheds light on the origin of
872 metazoan multicellularity. *Dev. Biol*. **377**, 284-292 (2013).

873 55. Booth, D., Middleton, H. & King, N. Choanoflagellate transfection illuminates their cell
874 biology and the ancestry of animal septins. *Mol. Biol. Cell*. **29**, 3026-38 (2018).

875 56. Wetzel, L. A., Levin, T. C., Hulett, R. E., Chan, D., King, G. A., Aldayafleh, R., Booth, D.
876 S., Sigg, M. A. & King, N. Predicted glycosyltransferases promote development and
877 prevent spurious cell clumping in the choanoflagellate *S. rosetta*. *eLife* **7,** e41482 (2018).

878 57. Chen, J. E., Barbrook, A. C., Cui, G., Howe, C. J. & Aranda, M. The genetic intractability
879 of *Symbiodinium microadriaticum* to standard algal transformation methods. *PLoS ONE*
880 **14,** e0211936 (2019).

881 58. Waller, R. F., Cleves, P. A., Rubio-Brotons, M., Woods, A., Bender, S. J., Edgcomb, V.,
882 Gann, E. R., Jones, A. C., Teytelman, L., von Dassow, P., Wilhelm, S. W. & Collier, J. L.
883 Strength in numbers: collaborative science for new experimental model systems. *PLoS*
884 *Biol*. **16**, e2006333 (2018).

885

886

887 **FIGURE LEGENDS**

888

889 **Fig. 1. | Phylogenetic relationships and transformation status of marine protists.** A
890 phylogenetically-informed approach was used to select protists for concerted genetic
891 manipulation efforts. A schematic view of the eukaryotic tree of life with effigies of main
892 representatives. Colour-coordinated species we have attempted to genetically modify, are
893 listed below. Current transformability status is schematized in circles indicating: DNA
894 delivered and shown to be expressed (yellow; for details see text and Table 1); DNA
895 delivered, but no expression seen (grey); no successful transformation achieved despite
896 efforts (blue). The details of transformation of species that belong to “DNA delivered” and
897 “Not achieved yet” categories are described in the Supplementary Data. Delivery methods
898 and construct types are shown pictorially. Overall, protocols and specific reagents are

available to transfect 22 protist species belonging to 7 eukaryotic supergroups, for 14 species we show first succesful attempt of either stable or transient transformation, for 7 species an alternative transformation or improvement of existing transformation protocol is shown and for 1 species we review an already published or existing protocol.

Fig. 2. | Epifluorescence micrographs of transformed marine protists

Transformants and wild-type cell lines of 10 selected protist species. Colored boxes behind species names refer to phylogenetic supergroup assignments given in Fig. 1. For each of these fluorescence micrographs details of transformation protocol as well as a second form of evidence are described in the Results and summarized in Table 1.

Scale bars are as follows: 10 µm for *A. amoebiformis*, *T. pseudonana*, *A. limacinum*, *B. saltans*, *N. gruberi*, *A. whisleri*, and *S. rosetta*; 15 µm for *P. marinus*; 20 µm for *F. cylindrus*; 100 µm for *P. multiseries.*

Fig. 3. | Various methods were used to demonstrate successful transformation in different species.

Luminescence, Fluorescence (by FACS and epifluorescence), Western blot, RT-PCR or sequencing (in case of Cas9-induced excision by CRISPR) were used to verify the expression of introduced constructs in three Archaeplastids (**a, b, c**), one Haptophytan (**d**), one Rhizarian (**e**), two Stramenopiles (**f, g**), three Alveolates (**h, i, j**), two Discobans (**k, l**) and one Opisthokont (**m**). Note that *nptII / neo* is used synonymously with amino 3'-glycosyl phosphotransferase gene (*aph(3')*) conferring resistance to kanamycin, neomycin, paromomycin, ribostamycin, butirosin and gentamicin B. (**a**) *In vivo* luminescence of 8 *O. lucimarinus* G418-resistant transformants depicted as relative luminescence unit (RLU) per 5 s and a corresponding gel showing PCR amplification from DNA of transformants of the

whole *pH4:KanMX pHAPT:luc* transgene. A band of the expected size was amplified in all transformants and absent in WT (control cells electroporated without constructs) and the PCR negative control (H_2O). (**b**) *In vivo* luminescence of 14 *B. prasinos* transformants resistant to G418 depicted as RLU per 5 s and a corresponding gel showing PCR amplification from DNA of transformants of *pH4:KanMx* (primers 1 and 2) and *pHAPT:luc* sequences (primers 3 and 4). (**c**) FACS analysis of *M. commoda* cells in two treatments: controls (wild type [WT] or "no-pulse", in which *eGFP* constructs were added but no electroporation pulse applied), and in the treatment to which the pulse was applied ("Transformed"). Note that lower panels include only the population of healthy cells selected using the depicted gates in upper panels. No compensation was used and PMT voltages were identical. Bar graphs show the mean and standard deviation of eGFP fluorescence from biological triplicates in the same experiment, analyzed as control (WT, i.e., "no-pulse" on cultures with constructs present) and pulsed (EW-113 treatment, with cells in the latter treatment analyzed as non-transformed, all eGFP and high eGFP (cells for which eGFP fluorescence was an order of magnitude higher than controls). Transformation efficiencies also reflect mean and standard deviations of biological triplicates. Images show natural chlorophyll fluorescence (red, top left), eGFP (green, top right) from a transformed cell (indicated by white arrow in all panels), with DAPI DNA staining (blue, bottom left), and the overlay of all three (bottom right) demonstrating the eGFP fluorescence is localized to the nucleus as designed. The scale bar represents 5 μm. (**d**) Expression of nourseothricin N-acetyl transferase (*nat*) in pIgNAT transformed *I. galbana*, from cells exhibiting resistance to nourseothricin. Expression of the *nat* transgene in WT (lane 3) and transformants (lanes 1 and 2) of *I. galbana* verified by RT-PCR. RT- negative and no template controls are shown in lanes 4 and 5, respectively, and 50 bp ladder (Bioline, lane 6), positive control PCR of genomic DNA from transformed cells (lane 7). (**e**) Western blot of expressed eGFP in *A. amoebiformis*, with total proteins extracted from transformants

(TF) and WT cells using α-GFP monoclonal antibody (Takara; 1:1,000), and an α-mouse horseradish peroxidase (HRP)-coupled antibody (GE Healthcare; 1:10,000). (**f**) Expression of *eGFP*, *ShBle* and *Rhodopsin* (endogenous gene used as control) in WT (lane 2) and transformants (1350 FC2: lane 4, 1100 FC2: lane 6) of *F. cylindrus* verified by RT-PCR. RT- negative controls are shown in lanes 3, 5 and 7. The NEB 100 kb ladder is shown in lane 1. (**g**) Cas9-induced excision of a 38-bp region in the *cGOGAT* gene (Phatr3_J24739). The sequence alignments from 10 *P. tricornutum* mutants (24739 KO-1 to KO-10) and two WT cell lines are shown. The two sgRNA target loci (g24739-A and g24739-B) are shown by green bars and include both the 20-nt sequence loci and the 3-nt PAM (protospacer-adjacent motif) sequence. The Cas9 double-stranded break sites are represented by the red rectangle. The predicted excision genotype is shown and represents the excision by dashes; the 38-bp excision is followed by an in-frame TGA stop codon. The excision/mutagenesis frequency is shown in the table below. (**h**) RT-PCR of the *nptII / neo* gene in kanamycin resistant *K. veneficum* transformants. No template negative control (lane 1); RT- negative controls of WT and transformed cells (lanes 2 and 4, respectively); cDNA from WT cells grown without antibiotics (lane 3), cDNA from transformants grown under kanamycin selection (lane 5), PCR positive control using the original vector DNA (DinoIII-*neo*, lane 6), GeneRuler DNA ladder (lane 7). Nothing was loaded in lane 8. cDNA libraries were made with 200 ng of RNA from WT and CA-137 transformant and all PCRs were nested. (**i**) Western blot of expressed MOE-GFP in *P. marinus* transformants. Cells subjected to electroporation without the plasmid present (MOCK) and WT were included as controls. Polyclonal rabbit α-GFP antibody (Invitrogen; 1:1,000) and secondary goat α-rabbit HRP-coupled antibody (Invitrogen; 1:10,000) were used for visualization. Polyclonal rabbit α-histone H3 antibody (Invitrogen; 1:1,000) was used as a loading control. (**j**) RT-PCR verification of *A. carterae* transformants showing transcription from an artificial minicircle based on *atpB*. HyperLadder

974 1 kb plus (lane 1), positive control PCR with artificial minicircle template (lane 2), negative
975 control with no template (lane 3), RT-PCR against chloramphenicol acetyltransferase (*cat*)
976 transcript from artificial minicircle (RT+, lane 4), RT-PCR against *cat* transcript from
977 artificial minicircle (RT- negative control, lane 5). (**k**) RT-PCR confirming expression of
978 *nptII / neo* gene expression in *B. saltans* transformants. GeneRuler 1 kb DNA Ladder (lane
979 1), *nptII / neo* expressed in *B. saltans* cells transformed with EF-1 alpha plasmid (lane 2);
980 RT- negative control from transformed *B. saltans* cells (lane 3), PCR for the EF -1 alpha
981 plasmid on RNA after DNase treatment (to verify absence of DNA, lane 4), PCR positive
982 control using the EF- 1 alpha plasmid DNA (lane 5), negative control with no template (lane
983 6). (**l**) Western blot of *D. papillatum* WT and C5 and C4 transformants that express the V5-
984 tagged *nptII / neo* gene. Monoclonal mouse α-V5 antibody (Invitrogen; 1:2,000) and
985 secondary α-mouse HRP-coupled antibody (Sigma; 1:1,000) were used. V5-tagged-
986 mNeonGreen *Trypanosoma brucei* cells served as a positive control and mouse α-alpha-
987 tubulin antibody (Sigma; 1:5,000) was used as a loading control. (**m**) For top and bottom
988 gels, RT-PCR of *A. whisleri* cells transfected with either 1 μg pAwhi_H2Bvenus vector plus
989 10 mg carrier DNA (pUC19) (lanes 1-3), carrier DNA only (lane 4) or without DNA (lane 5),
990 and pAwhi_H2Bvenus used as positive control (lane 7). A 1 kb DNA ladder was used (lane
991 6).
992
993 **Fig. 4. | 'Transformation Roadmap' for the creation of genetically tractable protists.**
994 (**a**) **Vector design and construction**. The three main goals for transformation of protists or
995 other taxa are: 1) to determine an appropriate selection marker, 2) to design a suitable
996 construct and 3) to find an appropriate transformation method for delivering DNA. Examples
997 from this research exhibited different levels of success many with DNA delivered and
998 expressed but ranging to DNA delivered without confirmation of gene expression or DNA

delivery not yet achieved (see **Fig. 1**). (**b**) **Transformation approaches**. Different symbols represent methods (e.g. chemical, physical or biological) for introducing DNA/RNA/protein into a living cell. (**c**) **Protocol**. Key methodological steps for successful transformation are listed in an abbreviated form (for particular examples, see table 1 and text).

Fig. 1

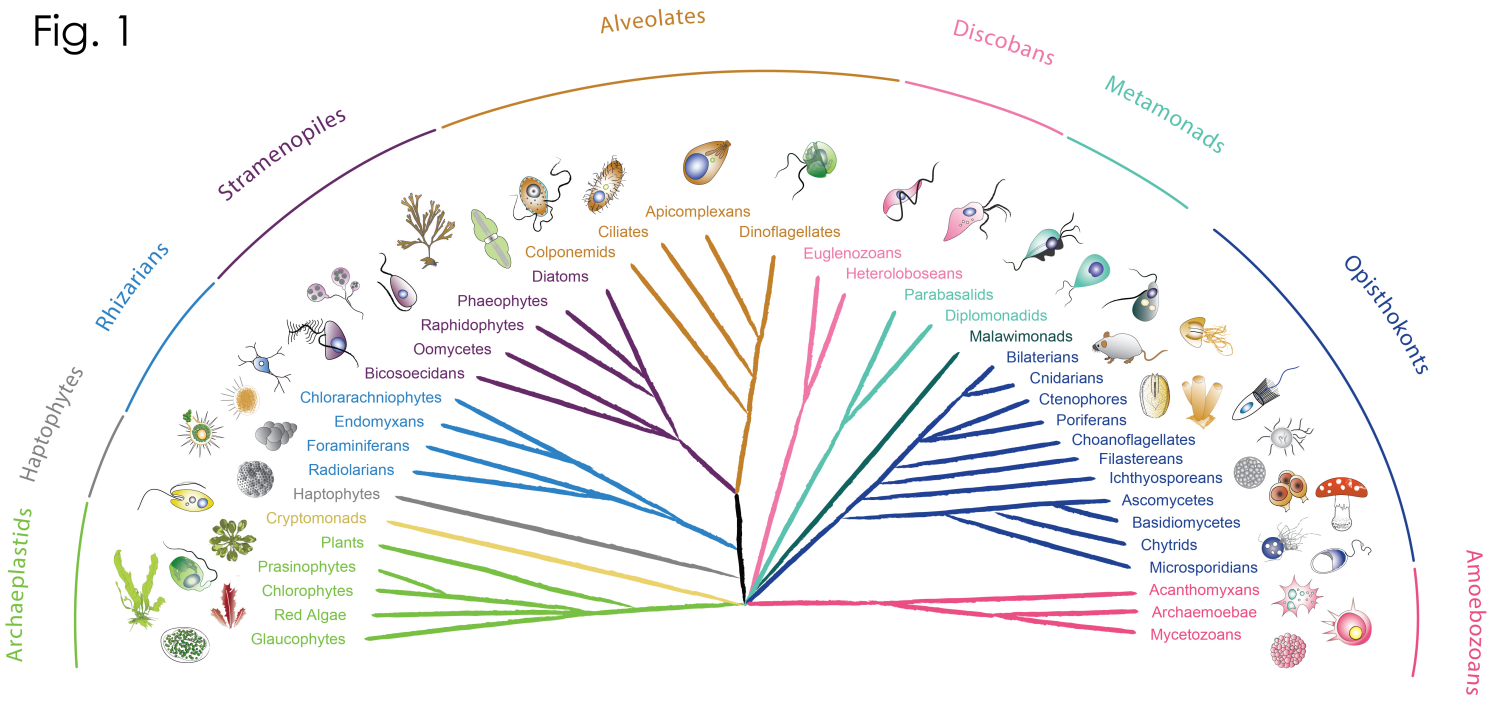

Archaeplastids

Ostreococcus lucimarinus	A		R
Bathycoccus prasinos	A		R
Micromonas commoda	A		
Micromonas pusilla			
Tetraselmis striata	A		R
Pyramimonas parkeae			

Haptophytans

Isochrysis galbana	A		R
Emiliania huxleyi			

Rhizarians

Amorphochlora amoebiformis	B^{25}		
Bigelowiella natans			

Stramenopiles

Fragilariopsis cylindrus	A		R
Thalassiosira pseudonana	$B^{15,17}$		R
Seminavis robusta			
Pseudo-nitzschia multiseries	A		R
Heterosigma akashiwo			
Aurantiochytrium limacinum	B^{31}		R
Caecitellus sp.			
Nannochloropsis oceanica	A		
Phaeodactylum tricornutum	$B^{15,18}$		R

Alveolates

Euplotes crassus			
Euplotes focardii			
Chromera velia			
Perkinsus marinus	$B^{44,45}$		R
Oxyrrhis marina	A		
Hematodinium sp.			
Fugacium (Symbiodinium) kawagutii			
Alexandrium catenella			
Breviolum (Symbiodinium) sp.			
Crypthecodinium cohnii	A		
Amphidinium carterae (chloroplast)	B^{40}		R
Karlodinium veneficum	A		R

Discobans

Bodo saltans	A		R
Diplonema papillatum	B^{51}		R
Eutreptiella gymnastica			
Naegleria gruberi	A		R

Opisthokonts

Pirum gemmata			
Sphaeroforma arctica			
Abeoforma whisleri	A		
Salpingoeca rosetta	$C^{55,56}$		R

Natural Communities

Pico-Eukaryotes	A		

TRANSFORMATION STATUS

- DNA delivered and expressed
- DNA delivered
- Not yet achieved

A First successful transformation of a particular species

B Alternative transformation / or improvement of the existing transformation method

C Review of an already published / existing protocol

CONSTRUCT

- Homologous
- Heterologous
- Labeled DNA
- mRNA
- FITC–Dextran

DELIVERY SYSTEM

Chemical · Electroporation · Conjugation · Biolistics · Glass beads abrasion · Microinjection

R Resistance selection · CRISPR/Cas9 · Did not work

Fig. 2

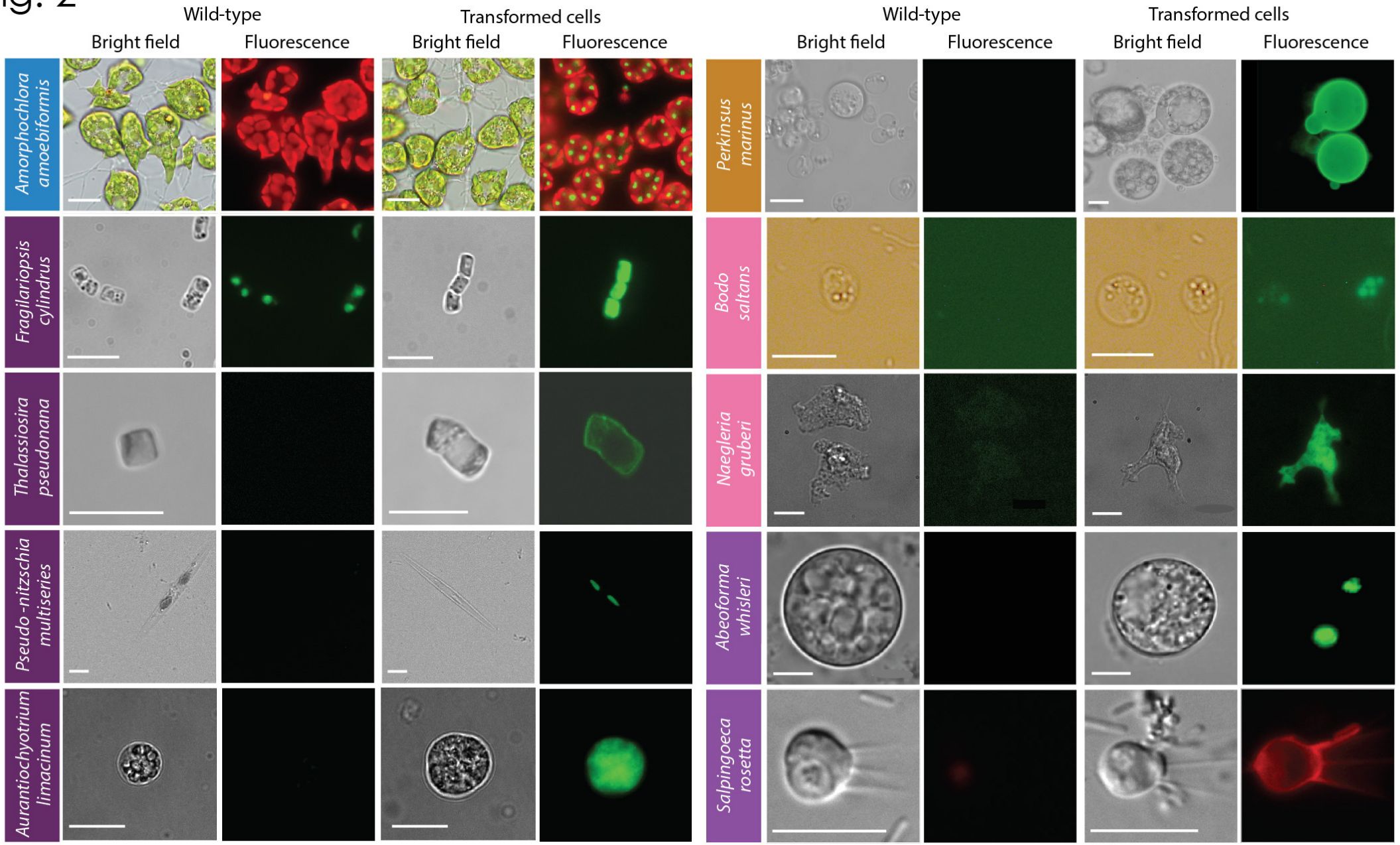
Wild-type
Transformed cells
Wild-type
Transformed cells
Bright field
Fluorescence
Bright field
Fluorescence
Bright field
Fluorescence
Bright field
Fluorescence
Amorphochlora amoebiformis
Fragilariopsis cylindrus
Thalassiosira pseudonana
Pseudo -nitzschia multiseries
Aurantiochytrium limacinum
Perkinsus marinus
Bodo saltans
Naegleria gruberi
Abeoforma whisleri
Salpingoeca rosetta

Fig. 3

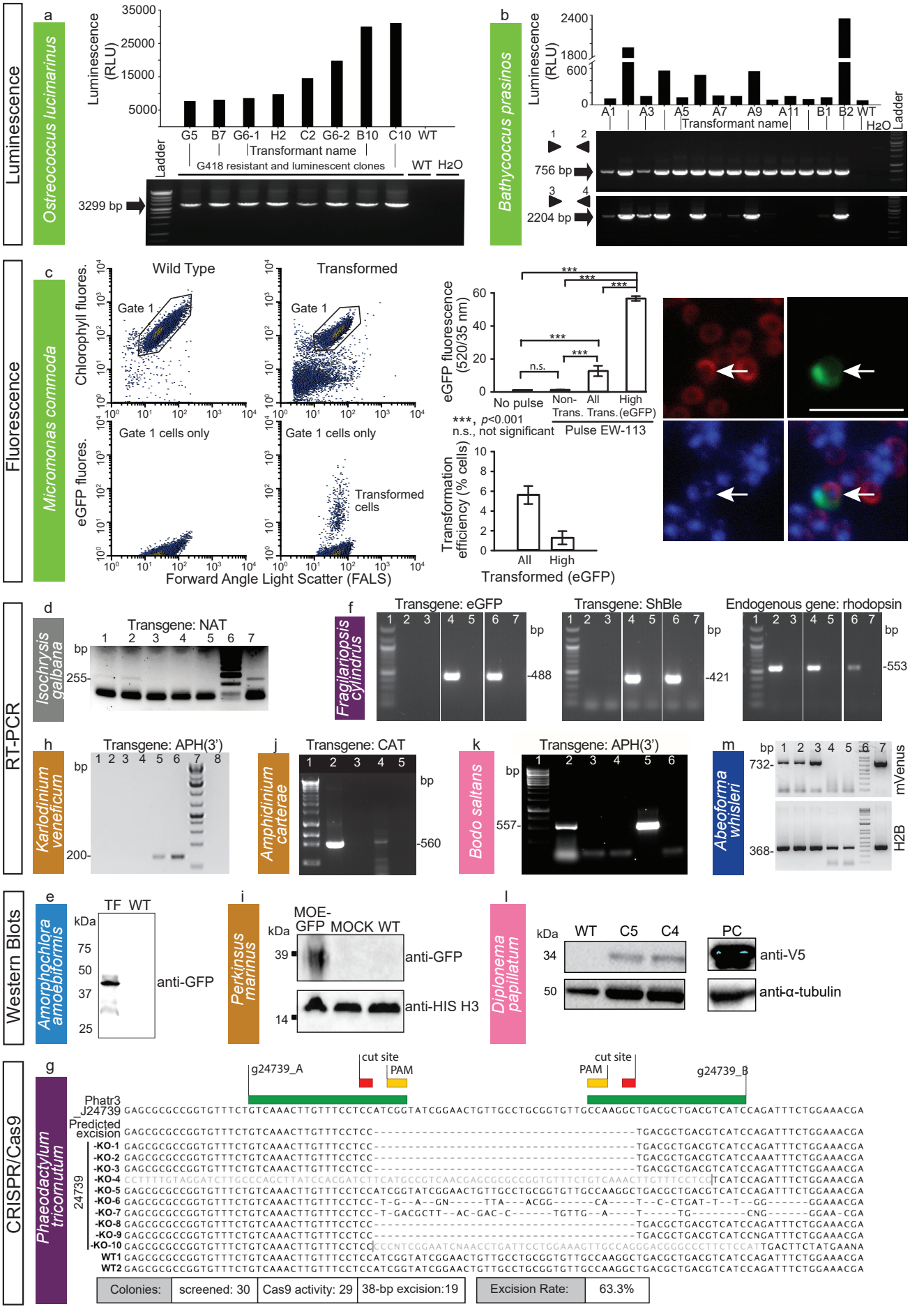

Fig. 4

a

Vector construction

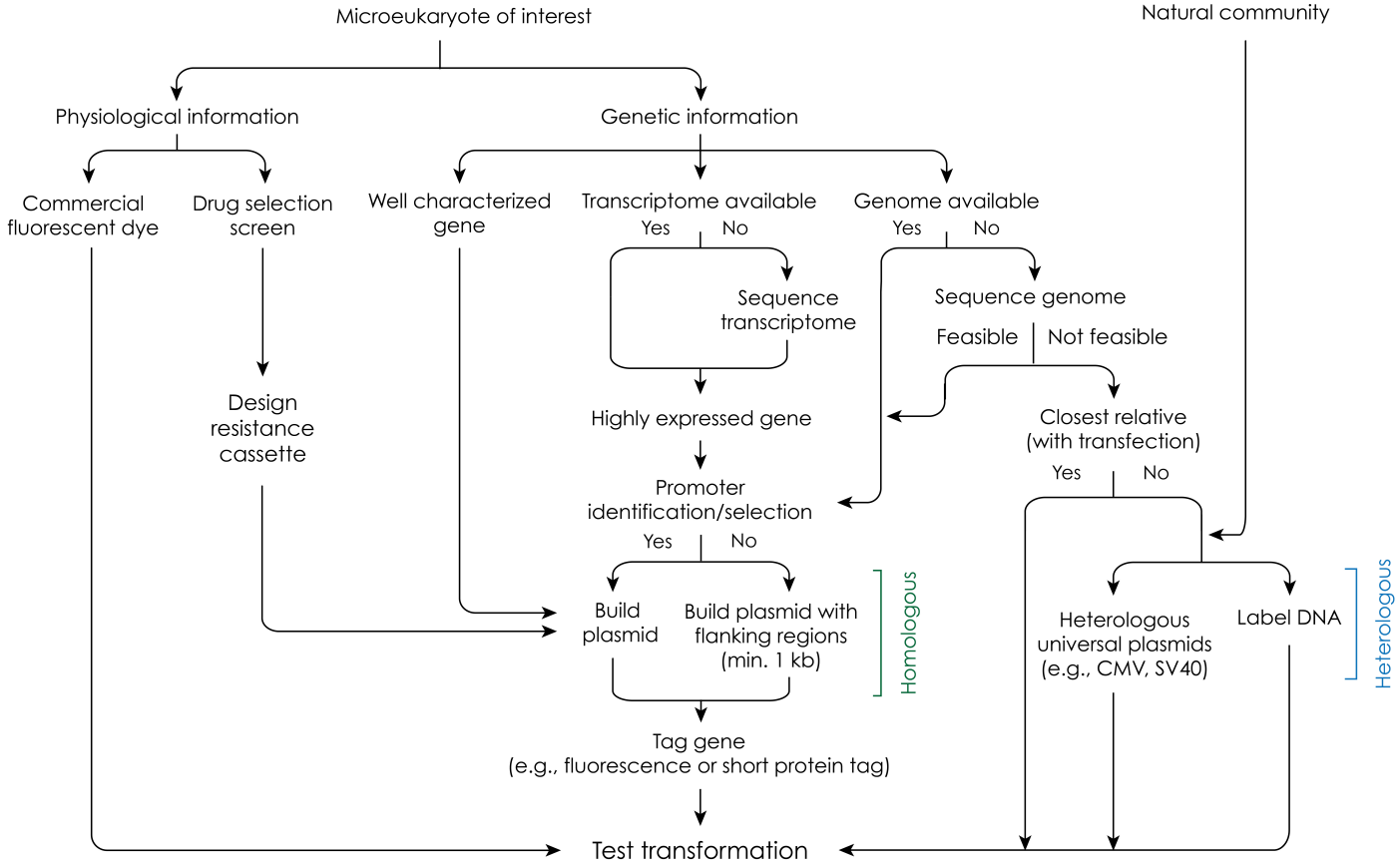

b

Transformation approaches

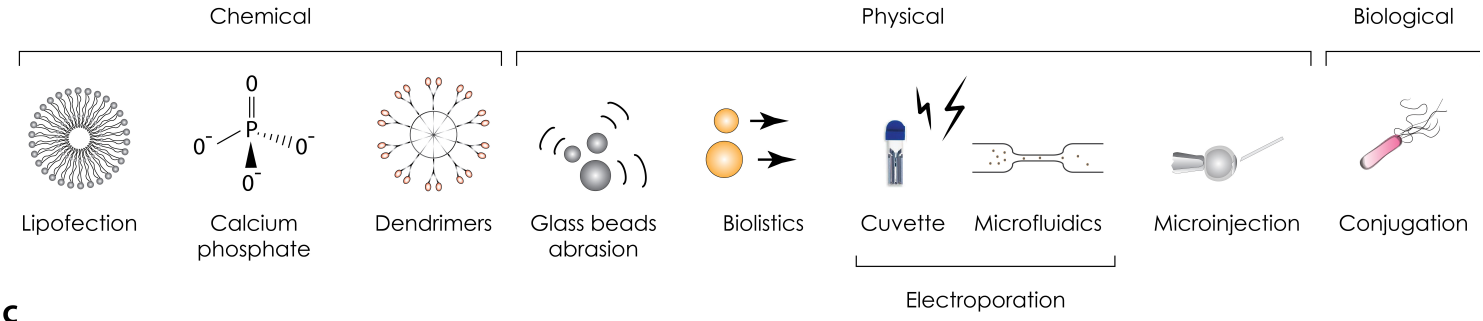

c

Protocol

Organism

- Description (life cycle stages)
- Strain
- Growth conditions and media
- Maximum cell density
- Autofluorescence
- Genome/transcriptome availability
- Cryopreservation

Resistance markers

- Antibiotics tested
- Assay used
- Resistance/sensitivity (IC_{50})

Constructs

- Construct name
- Origin
- Annotation
  - Promoter
  - UTRs
  - Flanking regions
  - Resistance
- Nature
  - Autonomously replicating
  - Integrative
  - Transiently

Transformation

- Method
- Parameters
  - Buffer composition
  - Program
- Cell stage and density
- DNA concentration
- Drug selection
  - Concentration
  - Time
- Efficiency

Transformants

- Clones examined
- Proof of nucleic acid uptake
  - Isolation of total DNA
  - PCR verification
  - Southern blot
- Plasmid maintenance
  - Chromosomal integration
  - Episomal
- Transcription
  - RT-PCR
  - Northern blot
- Translation
  - Western blot
  - Epifluorescence microscopy
  - Protein localization
- Phenotype
  - Growth curve
  - Description

Table 1: Parameters used for successful transformation as shown in Figs. 2 and 3.

For additional information, see protocols.io, Suppl. table 5, and Suppl. doc.1. For contacting laboratories working with particular species, see details given in Suppl. table 6.

Species	Transformation Method/ Device	Cell number	Vector;Amount (µg)	Promotor	Regulatory elements	Drug selection (µg/ml)	Time selection (Day)	Efficiency (%)	Transformation status (Stable/ Transient)	Reporter	Evidence of transformation	protocols.io link
Archaeoplastids												
Ostreococcus lucimarinus (RCC802)	Electroporation Genepulser II	1-2x10^9	Plasmid PotLuc; Linear; 5	HAPT, Histone H4 *O. tauri*	None	G418 (1000)	10-21	<0.0001	S	Luc	G418 resist, Luminescence, PCR	https://www.protocols.io/view/selection-of-stable-transformants-in-ostreococcus-zj2f4qe https://www.protocols.io/view/transient-luciferase-expression-in-ostreococcus-ot-hcib2ue https://www.protocols.io/view/transient-transformation-of-ostreococcus-species-o-g86bzze
Bathycoccus prasinos (RCC4222)	Electroporation Genepulser II	1-2x10^9	Fusion PCR; *p*HAPT: *p*LucpH4:KanM; Linear; 5	HAPT, Histone H4 Endogenous	None	G418 (1000)	10-21	<0.0001	S	Luc	G418 resist, Luminescence PCR	http://dx.doi.org/10.17504/protocols.io.g86bzze http://dx.doi.org/10.17504/protocols.io.zj2f4qe http://dx.doi.org/10.17504/protocols.io.hcib2ue
Micromonas commoda (CCMP 2709)	Electroporation Lonza-Nucleofector	3 x 10^7	RPS9pro^{Mco}-eGFP-NLS-RPS9ter in pUC05-AMP; Circular; 10-20	Endogenous, ribosomal protein S9;	Endogenous, ribosomal protein S9;	n/a	2-6	5.6±1.3	T*	eGFP	Per cell eGFP Fluorescence, Fluorescence microscopy	http://dx.doi.org/10.17504/protocols.io.8p9hvr6
	Electroporation Lonza-Nucleofector	3 x 10^7	H3pro^{Mpo}-LUC-H3ter in pUC05-AMP; Circular; 10-20	Histone H3 5' UTR from *M. polaris*	Histone H3 3' end formation -histone stem loop from *M. polaris*	n/a	3	n/a (Luc. assay is bulk, not per cell)	T*	NanoLuc®	Luminescence	http://dx.doi.org/10.17504/protocols.io.8p8hvrw
Tetraselmis striata (KAS-836)	Biorad Biolistics PDS-1000/He biolistics system	2.0x10^7	pACTpro:Ble; Linear; 1.0	Actin, *T. striata*	Actin, *T. striata*	Zeocin (150)	21-28		S		Zeocin resist, PCR	http://dx.doi.org/10.17504/protocols.io.hjtb4nn
Haptophytes												
Isochrysis galbana (CCMP 1323)	Biolistics PDS-1000/He	1-2x10^6	*p*IgNAT; Circular; 1.0	Hsp70 *E. huxleyi*	Heterologous	Nourseothricin (80-150)	14	<0.0001	S	None	Nourseothricin resistance, PCR, RT-PCR	https://www.protocols.io/view/biolistic-transformation-of-isochrysis-galbana-2pugdnw https://www.protocols.io/view/method-for-electroporation-of-isochrysis-galbana-c-hmab42e
Rhizarians												
Amorphochlora (Lotharella) amoebiformis (CCMP 2058)	Electroporation Gene Pulser Xcell	0.5-1×10^7	GFP-Rubisco; Circular; 30-50	rbcS1, Endogenous	rbcS1 Endogenous	*Manual selection of fluorescent cells	n/a	n/a	S/T	GFP	Fluorescence, Western blot	http://dx.doi.org/10.17504/protocols.io.35hgq36
Stramenopiles												
Fragilariopsis cylindrus (CCMP 1102)	Biorad Biolistics PDS-1000/He biolistics system	5x10^7	pUC:FCP:ShBle:FCP:eGFP; Circular; 1.0	FCP, Endogenous	None	Zeocin (100)	21 – 49	0.00003 (30 cfu/10^8 cells)	S	eGFP	Zeocin resist, Fluorescence, PCR, RT-PCR	http://dx.doi.org/10.17504/protocols.io.z39f8r6 https://www.protocols.io/view/biolistic-transformation-of-polar-diatom-fragilari-z39f8r6
Thalassiosira pseudonana (CCMP 1335)	Bacterial conjugation	4x10^7	TpSil3p-eGFP in pTpPuc3; Circular; n/a	Endogenous	Endogenous	Nourseothricin (100 in plates, 200 in liquid culture)	~14	~10	T	eGFP	Nourseothricin resistance, colony PCR, fluorescence	http://dx.doi.org/10.17504/protocols.io.nbzdap6 http://dx.doi.org/10.17504/protocols.io.7ghhjt6
Pseudo-nitzschia multiseries	Conjugation	1x10^5	Pm_actP_egfp_actT; pPtPUC3	Pm actin; Pt fcpB,	None, other than contained in Promoter/term	Manual selection,of fluorescent cells in LGTA; zeocin [200],	24h, 7	<0.1%	T	eGFP, shble	Fluorescence, vector targeted PCR on gDNA	http://dx.doi.org/10.17504/protocols.io.4pzgvp6
Aurantiochytrium limacinum (ATCC MYA-1381)	Bio – Rad Gene Pulser (165-2076) NEPA21	1×10^8	18GZG 18GeZG plasmid; Linear; 1-10	Endogenous GAPDH	None	Zeocin (100)	5-7	44 per µg of DNA	S	eGFP, shble	Zeocin resist., PCR, Southern, Fluorescence	http://dx.doi.org/10.17504/protocols.io.8xyhxpw
Nannochloropsis oceanica (CCMP 1779)	Electroporation Genepulser II	1x10^9	pMOD, Linear/Circular; 0.1-1	CMV	None	None	0.1-1	20 (linear) 1-2 (circular)	T	mTagBFP2	Fluorescence, PCR, RT-PCR	http://dx.doi.org/10.17504/protocols.io.h3nb8me

Phaeodactylum tricornutum (CCAP1055/1)	Bacterial-conjugation	$4x10^7$	hCas9-2A-shble PtpBR episome 100uL E.coli OD_{600}=0.9	FcpF-hCas9 psRNA-sgRNA	Cen6-Arsh4-His3 centromere	Phleomycin (50) Zeocin (100)	10-16	$1.25e^{-5}$ ~500 cfu	S	shble (Cas9) yfp VENUS	Phleoycin resistance, PCR maintained episome, PCR Cas9 target site	http://dx.doi.org/10.17504/protocols.io.4bmgsk6 http://dx.doi.org/10.17504/protocols.io.7gihjue http://dx.doi.org/10.17504/protocols.io.7gnhjve
Alveolates												
Perkinsus marinus (ATCC PRA240)	Electroporation LONZA-Nucleofector Glass beads abrasion (425-600 µm)	$5-7x10^7$	*p*PmMOE-GFP; Linear-Circular (1:1); 5	Endogenous	Endogenous	FACS Blasticidin(50-200) Puromycin (10-50) Bleo (50-200)	Drug: 20-60 FACS: 3	0.01-5	S	GFP, mCherry	Fluorescence Sequencing, PCR, Western blot	https://www.protocols.io/view/oyster-parasite-perkinsus-marinus-transformation-u-gv9bw96 https://www.protocols.io/view/glass-beads-based-transformation-protocol-for-perk-g36byre https://www.protocols.io/view/fluorescence-activated-cell-sorting-facs-of-perkin-hh2b38e
Oxyrrhis marina (CCMP 1788, CCMP 1795)	Electroporation Gene Pulser Xcell; Chemical ($CaCl_2$)	$1-5×10^6$ $1x10^5$	Fluorescently labelled DNA (5-25 µg) or FITC-dextran; mCherry	n/a Endogenous hsp90	n/a Endogenous hsp90	n/a	n/a	0.5-5%	T	mCherry	Fluorescence	https://www.protocols.io/view/electroporation-of-oxyrrhis-marina-vcne2ve https://www.protocols.io/view/transfection-of-alexa488-labelled-dna-into-oxyrrhi-ha8b2hw https://www.protocols.io/view/electroporation-transformation-of-fitc-dextran-int-3cmgiu6 https://www.protocols.io/view/co-incubation-protocol-for-transforming-heterotrop-hmzb476
Crypthecodinium cohnii (CCMP 316)	Electroporation LONZA-Nucleofector		Stained DNA (739 bp); Linear; 1	None	None	n/a	n/a	<0.001	T	Fluorescence	Fluorescence	https://www.protocols.io/view/transfection-of-crypthecodinium-cohnii-using-label-z26f8he
Amphidinium carterae (chloroplast) (CCMP 1314)	Biorad Biolistics PDS-1000/He biolistics system	$2.5x10^7$	*p*AmpAtpBChl; Circular; 0.5	Endogenous	Endogenous	Chloramphenicol (20)	3 onwards	n/a	S	Ab res	RT-PCR, PCR Phenotype	http://dx.doi.org/10.17504/protocols.io.4r2gv8e
Karlodinium veneficum (CCMP 1975)	Electroporation	$4x10^5$	linear-DinoIII-neo; Linear; 2	Endogenous	Endogenous	Kanamycin (150)	7	0.0005	S (3 mon)	n/a	RT-PCR, PCR	https://www.protocols.io/view/nucleofector-protocol-for-dinoflagellates-using-lo-qm8du9w
Discobans (Euglenozoans and Heteroloboseans)												
Bodo saltans (submitted to ATCC)	Electroporation Nepa21	$1-1.5x10^7$	Bs-EF1- a C- terminal tagging; Linear; 3-5	Endogenous	Endogenous	G418 (3)	7-9		S	GFP	Fluorescence, PCR, RT-PCR	http://dx.doi.org/10.17504/protocols.io.s5jeg4n http://dx.doi.org/10.17504/protocols.io.7fchjiw
Diplonema papillatum (ATCC 50162)	Electroporation LONZA-Nucleofector	$5x10^7$	*p*57-V5+Neo^R; Linear; 3	Endogenous	Endogenous	G418 (75)	7-14	~5.5	S	n/a	Western blot (resistance marker), RT-PCR	http://dx.doi.org/10.17504/protocols.io.4digs4e
Naegleria gruberi (ATCC 30224)	Electroporation BioRad Gene Pulser xCell	$5x10^6$	*p*NAEG-HYG; Circular; 4	Endogenous	Endogenous	Hygromycin (300) Neo (700)	15-28	80	T	GFP	Western blot (resistance marker), Fluorescence,	http://dx.doi.org/10.17504/protocols.io.hpub5nw http://dx.doi.org/10.17504/protocols.io.7w4hpgw
Opisthokonts												
Abeoforma whisleri (ATCC PRA-279)	Electroporation LONZA-Nucleofector	$3x10^5$	Awhis_H2Bvenus+ *p*UC19; Circular; 1-5+ 40 carrier	Endogenous	Endogenous	n/a	10-15	1	T	Venus	Fluorescence, RT-PCR	http://dx.doi.org/10.17504/protocols.io.zexf3fn
Salpingoeca rosetta (ATCC PRA-390)	Electroporation LONZA-Nucleofector	$4x10^5$	SrActmCherry-CCTLL + *p*UC19; Circular; 1-10 + 40 carrier	Endogenous	Endogenous	Puromycin (80)	10-12		S	mCherry	Gene Expression (Luc, Fluorescen-ce)/resistance	http://dx.doi.org/10.17504/protocols.io.h68b9hw

*may be stable but overgrown by wild-type strain

Abbreviations: n/a, not applicable; NLS, Nuclear Localization Signal